FACULTY OF SCIENCE AND TECHNOLOGY

MASTER'S THESIS

Study programme / specialisation: Engineering Structures and Materials/ Structural Engineering	The spring semester, 2023 Open / ~~Confidential~~
Author: Ida Moen	
Supervisor at UiS: Associate Prof. Yanyan Sha Co-supervisor: Mathias Eidem	
Thesis title: Analysis of a ship-bridge collision at Nordhordland Bridge	
Credits (ECTS): 30	
Keywords: Ship Collision Floating bridges Nordhordland Bridge Risk Assessment Finite Element Method LS-DYNA	Pages: 91 + appendix: 0 Stavanger, 15.06.23

Preface & Acknowledgements

This study is the concluding part of the Master´s Degree Programme Structures and Materials Engineering, with a specialization in Structural Engineering at the University of Stavanger. The work of the thesis has been conducted during the spring semester of 2023. Parts of the work in this thesis have been included in a scientific article that will be published for the coming European Safety and Reliability Conference in September 2023 [1]. This project is supported by the Norwegian Public Roads Administration.

First, I would like to thank my supervisor, associate prof. Yanyan Sha, and co-supervisor Mathias Egeland Eidem from the Norwegian Public Roads Administration, for support, whenever I had questions during this project and for the opportunity to be involved in the research regarding the risk assessment of Nordhordland Bridge. Your help and guidance about the subject have been very valuable and I am truly grateful.

Thanks to fellow students in structural engineering at UiS. The collaboration has brought us through these 5 years of studies. And a special thanks to fellow student and friend, Katrine Idsø, for working with LS-DYNA together with me during this project.

I also want to give a special thanks to DynaMORE, my contact person Axel Hallén, and to Sigma2. DynaMORE conducted a very informative intro course about the software LS-DYNA and provided help directly with the Finite Element Model for my thesis research. And thanks to Sigma2 - the National Infrastructure for High-Performance Computing and Data Storage in Norway, for providing the resources needed to simulate the numerical analyses with HPC FRAM in this research.

University of Stavanger

Stavanger, June 2023

Ida Moen

Abstract

The Nordhordland Bridge, a floating bridge located in Norway, spans a length of 1246 meters and was completed in 1994. Over the years, the bridge has experienced two instances of ship collisions so far, resulting in minor damage. Considering the advancements in ship collision risk assessment, ship impact analysis, and changes in ship traffic, a reassessment of the original design requirements for the bridge is undertaken. The main objective of this research is to determine if the prestressed reinforced concrete pontoons of the bridge have the strength to withstand accidental loading from a ship collision. As ship collisions pose a significant risk to the structural integrity of floating bridges, it is important to state the capacity of the pontoons. The impact of a ship collision can cause severe damage to the pontoons, leading further to a potential collapse of the bridge.

A structural impact analysis is carried out using the software LS-DYNA to assess whether the pontoons of the bridge can endure the previously determined impact load level. Five different scenarios are simulated in the analysis. A head-on impact in the centre of the pontoon, with and without a strengthening sheet of Carbon Fibre Reinforced Polymer (CFRP) of different thicknesses. A head-on impact off the centre of the pontoon, towards one of the internal concrete walls in the pontoon and a glancing blow will be analysed.

The results of the analysis indicate that the current pontoon design does not possess sufficient structural capacity to withstand the loads from a head-on ship impact, which amounts to approximately 25 MJ of impact energy. Additionally, it is evident that the extent of damage varies considerably depending on the specific location of the ship's bow impact with the pontoon. The results with the CFRP sheet strengthening the pontoon wall indicate a positive trend, suggesting that the approach employed may have a beneficial effect on the capacity.

The findings from the analysis reveal that the pontoons, which form the foundation of the bridge, are particularly vulnerable to ship impacts and do not possess adequate capacity to meet present-day requirements.

Keywords – Ship Collision, Floating Bridges, Nordhordland Bridge, Risk Assessment, Finite Element Method, LS-DYNA

Contents

List of Figures

List of Tables

1 Introduction

The Norwegian Public Roads Administration (NPRA) is planning a lot of new fjord crossings to be built along the Norwegian coast for the mission to get a ferry-free E39, all the way from Trondheim to Kristiansand as shown in Figure 1.1. Replacement of the current ferry crossings will reduce the travel time significantly, and an increase in traffic is expected as a result [2]. This will further promote growth in trade and business in cities and areas along the Norwegian coast. The project is challenging because of the distance of the crossings, and the great depth in many of the fjords. These challenges makes the options to cross some of the fjords narrow as conventional structures with fixed foundations becomes unfeasible. In these cases, floating structures will be a good option for the fjord crossings. With the technology available today, pontoon-supported floating bridges and submerged floating tunnels are the most considered floating options by the NPRA [2].

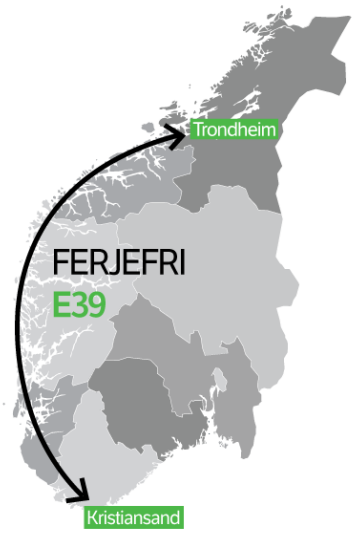

Figure 1.1: Ferry Free E39. Adapted from the NPRA [2]

When designing and constructing floating bridges and submerged tunnels, one of the main concerns is the ability to withstand structural damage on the floating elements, as a result of potential accidental loads. The floaters will often be the weakest element in the global bridge system, and in case of structural damage to the floaters, seawater can flow into the structure. This can lead to severe damage as the floater's buoyancy and stability decreases, and further lead to a collapse of the whole bridge installation. A total collapse can have tragic outcomes, both economic and environmental consequences and even a risk to human life. Hence, the structural design of the floating elements should be very conservative when designing a floating bridge or submerged tunnel.

In Norway, there are currently two floating bridges along the coast, but no submerged tunnels have been constructed so far. According to M. Lwin, a floating bridge is very cost-effective, as it is estimated to cost 3-5 times less than a fixed bridge, tube or tunnel

for a site where the water crossing is 2-5 km wide, 30-60 m deep and with a very soft seabed [19]. The existing floating bridges in Norway are the Bergsøysund Bridge near Kristiansund and the Nordhordland Bridge located right outside of Bergen. The focus of this thesis will primarily be on the Nordhordland Bridge, as is depicted in Figure 1.2. This bridge is a combination of a floating bridge consisting of prestressed reinforced concrete pontoons and a cable-stayed bridge.

The Nordhordland Bridge spans the Salhusfjord in the Bergen region, with water depths reaching up to 500 m [12]. It was initially opened in 1994 and, at that time, it was the longest floating bridge in Europe. Technologically, it posed a significant challenge with a total length of 1614 m, of which 1246 m comprises the floating section [12]. In comparison to the world's longest floating bridge, the Evergreen Point Floating Bridge, which has a floating span of 2350 m, the construction of the Nordhordland Bridge was quite an accomplishment for its time [19].

Figure 1.2: Overview of Nordhordland Bridge. Adapted from the NPRA [3]

The design codes for bridge structural design are continuously evolving with the introduction of new research and technology. Since the opening of the Nordhordland Bridge in 1994, the design codes used for its formation have undergone changes. Initially, the design process for the bridge incorporated NS 3472 for steel structures and NS 3474

for concrete structures, along with NPRA's Handbook 185 [12]. However, these NS codes have now been replaced by Eurocode (NS-EN 1993 and 1992), and the handbook has been updated to NRPA's Handbook N-400. Furthermore, over the years, there has been a shift in the philosophy of ship impact design, with greater emphasis placed on addressing this aspect.

There have been 2 accidents during the lifetime of Nordhordland Bridge so far, one in 2009 and in 2019. During the project with this thesis, a new ship collision occurred at Bergsøysund Bridge in March 2023. This bridge has a similar structural design as Nordhordland Bridge, with floating concrete pontoons. Although none of the ship collisions resulted in significant structural damage to the bridges, these incidents highlight the potential for such events to occur again, even in crossings with initially limited ship traffic.

As floating bridges are vulnerable to ship collisions, a risk evaluation is an important tool to manage safety, health and environmental protection. With an increase in ship traffic and in the size of vessels [20], it gets even more important to address and manage the potential risks caused by a ship-bridge collision. Hence, it is essential to study the bridge design and a potential ship-bridge collision to be aware of the potential risks.

1.1 Objective & Motivation

The objective of this thesis is to do an analysis of a ship collision at Nordhordland Bridge as a contribution to further work with risk and consequence assessment for the bridge. It will be performed a local analysis of the weakest point of the global bridge system, the floating pontoons. The analysis will review the impact response and capacity of the concrete pontoons during exposure to accidental loads. Several different impact scenarios will be considered to make it as realistic as possible. To achieve this, a numerical analysis will be performed by finite element method using the digital software, LS-DYNA. The proposed plan involves utilizing time to acquire experience in the software through an introduction course and training program organized by DynaMORE. The objective is to gain comprehensive knowledge and skills in utilizing the LS-DYNA software for various applications, but in particular for ship collisions.

The purpose of this study is to contribute to an investigation of the risk assessment of the pontoons of the bridge. This study is of interest because of the actual possibility of ship

collisions on existing bridges in real life. The hypothesis of the project is that the pontoon walls of Nordhordland Bridge most likely are undersized considering the requirements in the design codes used today, and may not be able to withstand a larger impact from a colliding ship without structural damage. The risk analysis can expose weaknesses in the structure that should be evaluated further, as it can pose a risk for human life, material and environmental damages and or large economic losses for the society. As the NPRA is planning several new projects in the years to come, the research may in addition contribute to innovation and development for new floating bridge projects as well.

1.2 Problem Statement

Analysis of a ship collision at Nordhordland Bridge, where several different ship impacts towards the pontoons of the bridge will be investigated using an FE-model in the software LS-DYNA. The impacts will vary with different incoming angles and positions of the ship. Risk evaluation will be performed where strengthening methods and procedures for dealing with high-risk impact will be proposed.

1.3 Limitations & Scope

It is important to acknowledge the limitations that may affect the scope of this thesis. The scope of this research narrows down to a local analysis of the impact isolated on the floating pontoons of the bridge. The analysis will consider only accidental loads from the ship impact in one of the pontoons. Neglecting other types of loads that the bridge could potentially encounter, such as dead loads, live loads, environmental loads, hydrostatics and hydrodynamics may restrict the comprehensiveness of the analysis and the response of the global bridge system will not be investigated. The design of the pontoon model in this research will have some simplification compared with the existing pontoons. Due to experience and skills in addition to time restrictions, the prestressing in the concrete pontoon is not included in the model. Complex computational models and simulations can require significant computational power and time, and simplification in the design and reduction of elements is necessary. These restrictions were set as time and computational capacity is considered to be a limitation for this thesis project.

The scope of the thesis is divided into eight chapters, each exploring a distinct aspect of

the research topic. A concise overview of each chapter is provided below:

Chapter 1: Presents an overview of the background for the research and gives a description of the problem statement, objectives and presents the structure of the thesis.

Chapter 2: Gives a brief review of the existing literature and research related to the research topic presented in this thesis. It investigates relevant theories, concepts, and previous studies, highlighting the gaps in the research that the thesis aims to address.

Chapter 3: The methodology implemented in the study is described in this chapter. Furthermore, a brief overview of relevant concepts of floating bridges.

Chapter 4: A detailed description of the design and material parameters of Nordhordland Bridge is introduced. The chapter also includes an investigation of local ship traffic, an assessment of the probability of ship collisions, and past ship collision incidents.

Chapter 5: Gives a detailed description of the analyse setup, and specifies the inputs utilized in the simulations.

Chapter 6: Presents the results and findings from the numerical analysis. The findings from the analysis are discussed in detail in this chapter. Challenges and possible errors affecting the simulations are addressed

Chapter 7: Serves the final conclusion of the research in the thesis, and presents suggestions for recommended further work.

2 Literature Review

The purpose of this chapter is to provide a brief qualitative description of the current research within ship-bridge collisions existing today, which this thesis will use as a baseline for further research. The literature review shows how the work in the thesis is related to existing research and what new insights the work presented in this thesis may contribute to.

The project started with getting familiarized with the existing research about ship-bridge collisions, design and structural analyses of floating bridges. To gather updated literature and knowledge related to risk assessment of floating bridges under ship collisions, several resources have been used. Relevant databases from the University Library of Stavanger, the NPRA and Google Scholar have provided many of the previous research papers, together with Standard Norge and standards from DNV GL.

From the literature review, it was found that Minorsky was the first to conduct a revealing study of ship collisions in 1958 [21]. The empirical formula related to absorbed energy proposed by Minorsky has been widely used when analysing high-energy collisions since [22]. Woisin [23] presented later, in 1979, a modified method of Minorsky´s research, and proposed a new formula based on a number of experiments of high energy collisions. The research provided by Minorsky and Woisin, in the form of experimental studies, has been essential for the understanding of the process of ship collisions today. Zhang [22] has presented an improvement for the methods presented by Minorsky and Woisin in his PhD research. The research done in the field has given good insights into the behaviour of structures with large deformation during a collision. Simplified formulas for estimating collision impact have been provided in codes widely used today, such as Eurocode, NORSOK and AASHTO.

Ship collisions have been further investigated with several studies since it first was introduced, especially in the past twenty years. These studies are often limited to ship-ship collisions and ship collisions with offshore structures. The literature review revealed that the literature including ship-bridge collisions is relatively narrow. Catastrophic ship-bridge collisions have occurred, where bridges have collapsed, disruption in traffic patterns, environmental damages and even people getting killed. An example of this was

the collapse of Almö Bridge in Sweden in 1980, where eight people died after a bulk carrier tore down the main span of the bridge [24]. The understanding of the consequences of a ship impact is crucial as the technology for bridge design is being constantly developed to more spectacular and complex bridge structures.

Consolazio at el [25] did experimental research by collisions between barge and bridge, with dynamic effects in 2006. As experimental analysis with realistic collisions is time-consuming and of high cost, numerical analysis as in an FE approach can rather be preferred. Yuan and Harik [26] investigated 3D numerical models of barges impact on bridge piers using the software LS-DYNA in 2008.

Sha and Amdahl are among the researchers in the Norwegian community that have further investigated ship-bridge collisions, and have published several papers of their research. In 2019 they proposed numerical investigations of prestressed pontoon walls subjected to ship impact [27]. In the study, the effect of prestressing was investigated. It concludes that prestressing will help to increase the collision resistance [27]. As one of the limitations of this thesis is that the concrete pontoon is without prestressing, the effects found by Sha and Amdahl will be implemented in the analysis.

Many methods for strengthening reinforced concrete structures against impact loads from collisions have been proposed in research papers. Sha and Hao [28] proposed in 2015 a method for reducing structural damage in bridge piers during barge bow collisions with CFRP composites. Sha [29] reported in 2022 further on how CFRP strengthening of RC pontoon walls against ship bow collision.

Most of the previous research presented on bridges is related to collisions near the navigation channel at fixed foundations or on the bridge girders. This thesis will contribute with analysis related to the floating parts specific to Nordhordland bridge, the pontoons, which has significantly smaller wall thickness than most of the research done earlier. There is a gap in the existing research to justify the content of the thesis, and the research will be a contribution to further research on risk assessment of existing floating bridges in Norway by co-supervisor Mathias Egeland Eidem. The technique for CFRP strengthening of RC pontoons in this thesis will be based on the research done by Sha [29] in 2022.

3 Methodology

The methodology will be presented in this chapter, where the theory and techniques for numerical analysis are described. This chapter will also describe some fundamental theories and knowledge related to and needed for the understanding of the structural design and analyses of floating bridges.

3.1 Review of Finite Element Method

Finite Element Method (FEM) is a method used to solve complex problems that usually are too complicated to be solved by classic analytical methods. By using numerical analysis to solve partial differential equations, complex problems can be solved by finite element analysis (FEA) to approximate the actual solution. By discretizing the geometry into small elements by mesh generation techniques, the variation of the solutions within the elements can be approximated using simple functions [30]. The collection of the solutions for all elements then forms the variation of solution for the whole complex problem [30].

The analysis consists of three parts:

- Pre-processing: Input data from the complex problem describes the geometry, material models, loads and boundary conditions. The model is being given a mesh to obtain more accurate solutions. Materials, sections and parts are defined with boundary conditions. Define desired output data. In other words, modelling.
- Numerical simulation: The software is generating matrices that describe the behaviour of the elements in the model. It solves the large matrix equation to determine the values of field quantities at nodes.
- Post-processing: The result can be listed or graphically displayed as an animation. Determination and examination of quantities of interest, such as stress, strain, deformation and energy.

The dynamic equation of motion can be solved by the dynamic response of a structure with respect to an external force. The equation of linear structural dynamics can be expressed as following [31]:

$$M\ddot{x} + C\dot{x} + Kx = R \tag{3.1}$$

where

M = mass matrix
C = damping matrix
K = stiffness matrix
R = external force vector
$\ddot{x}, \dot{x}, x$ = denotes the nodal acceleration

3.1.1 Nonlinear Analysis

Nonlinear analysis is an analysis where there is a nonlinear relation between the applied forces and the displacements in the structural problem. Nonlinear material behaviour in structural mechanics means that one or more of the following issues are present [31]:

Contact non-linearity: The boundary conditions are changing over time as the contact area between parts changes [31].

Geometric non-linearity: Large deformations in the structural geometry that needs to be considered in the equilibrium equations [31].

Nonlinear materials: materials properties are functions of the state of stress or strain. In other words, the material does not exhibit ideally elastic behaviour, but plasticity, nonlinear elasticity and creep [31].

When these effects are present, the stiffness matrix is not constant during the application of loads as it is in linear analysis. This results in that a different solving strategy needs to be considered for the nonlinear analysis as it is more complex than a linear analysis [30].

DNV-RP-C208 is a guidance on how to determine structural capacity by a nonlinear finite element analysis for marine steel structures [32]. The code is valid for marine structures made from structural steel meeting the requirements for marine environments with a yield strength of up to 500 MPa [32].

3.1.2 Elements in FEA

Element types utilized in FEA are strongly dependent on the problem to be solved [32]. High-order elements are normally preferred for precise stress estimates. Elements with simple shape functions, such as constant or linear functions, require a larger number of elements to attain the same level of stress accuracy as higher-order elements. It is not recommended to utilize constant stress elements in the designated area of interest [33].

Beam Elements consist of two nodes, with one located at each end. In the case of a 2D beam, each node possesses two degrees of freedom (d.o.f), lateral translation and rotation [31]. On the other hand, a 3D beam element has six d.o.f at each node, encompassing three translations and three rotations. The most prevalent theories for beams are the Euler-Bernoulli beam theory, elementary beam theory, and Timoshenko beam theory [31].

According to Euler-Bernoulli beam theory, the influence of transverse shear deformation can be disregarded when considering bending deformations. In contrast, Timoshenko beam theory takes into account transverse shear deformation alongside bending deformations [31]. A simple beam element is illustrated in Figure 3.1.

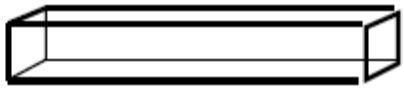

Figure 3.1: Beam Element. Adapted from [4].

Solid Elements have translations d.o.f in all nodes, and no rotations [34]. It can have any material properties, boundary conditions and arbitrary shape. A solid element can have six possible stress components, three normal and three shear components [30]. An illustration of shell elements is given in Figure 3.2.

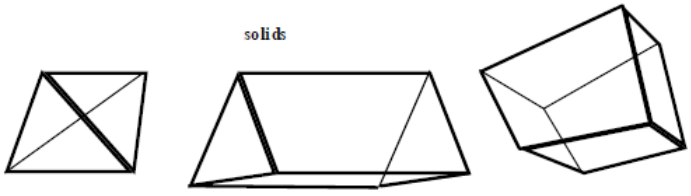

Figure 3.2: Solid Elements. Adapted from [4].

Shell Elements are usually triangular with three or six nodes, or rectangular with four or eight nodes. Each node with 6 d.o.f, three translations and three rotations [31]. A shell has a curved inner and outer surface, with a thickness that is relatively small compared with the overall dimension of the shell. The thickness of the shell can be constant or vary. Bending, twisting and membrane force is present in a shell element [31]. An example of shell elements is presented in Figure 3.3.

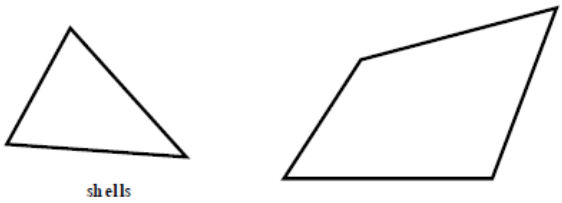

Figure 3.3: Shell Elements. Adapted from [4].

Hourglass Modes are non-physical, zero-energy modes of deformation that produce zero strain and no stress [34]. This is used when there is deformation in the elements, but no associated internal energy (zero-energy modes). This is for under-integrated solid and shell elements. This means that there is a single integration point in the mid-point of each element where the stresses and strains are calculated [34]. Then hourglass control needs to be used. A general rule is that the hourglass energy should be less than 10% of internal energy [34]. Hourglass energy in the FE model can be decreased by refining the mesh of the elements.

Proper element connectivity in the mesh should be established for elements next to each other. The element mesh has to be sufficiently detailed to be able to capture failures in the elements [30]. This is the Finite elements, small elements which are connected to each other. Given that numerical analysis methods provide only an approximation of complex systems, it is important to note that the accuracy of the solution increases as the number of elements employed in the analysis also increases [30]. However, the cost of computation time will also increase with the number of elements in the model.

3.1.3 LS-DYNA

LS-DYNA is an advanced simulation software used worldwide by industries like automobile, aerospace, civil engineering, military, manufacturing and bio-engineering to simulate real-world situations. It was developed by Livermore Software Technology Corporation (LSTC) in California, and was acquired by Ansys in 2019 [34].

The program is one of the most used software for nonlinear FEA for Accidental Limit State analysis. This involves drop tests, impacts, and crashes, among others. Complex models can be simulated as the program has many applications as elements, material models, contact and constraints formulations to control all the details in the simulation case [34]. Analysis capabilities of LS-DYNA are full 2D and 3D simulations, thermal analysis, fluid analysis, failure analysis, and nonlinear dynamics, to mention a few [35].

In LS-DYNA some element formulations are more accurate and more costly than others [34]. Among the many types of elements, beam, solid and shell elements are the most common elements in LS-DYNA.

LS-PrePost is an advanced graphical pre- and post-processor and model editor of LS-DYNA. In LS-PrePost text files can be imported, edited and exported, and generates input files to LS-DYNA [36].

In LS-DYNA there are two time integration methods, implicit and explicit analysis. From a practical point of view, the most significant difference between explicit and implicit analysis is related to stability and economy [31]. Figure 3.4 summarises the target areas for using implicit and explicit analysis considering non-linearity and velocity.

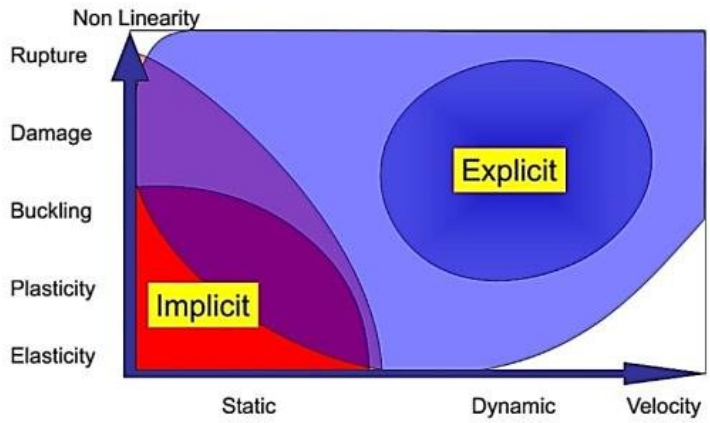

Figure 3.4: Implicit and explicit analysis [5].

An explicit analysis method employs a small time-step size and is conditionally [34]. This approach is suitable for short-duration transient events such as impacts or explosions in dynamic analysis. However, it can be computationally expensive when simulating loads with longer duration [34]. The explicit analysis method does not require matrix inversion or iterations.

In contrast to explicit analysis, implicit analysis adopts a larger time-step size. This results in fewer time steps being required for the analysis. However, each time step in implicit analysis typically incurs a higher computational cost [34]. An implicit analysis is particularly suitable for static analysis scenarios where the load changes slowly and has a longer duration [31]. Furthermore, implicit analysis can achieve unconditional stability.

3.2 Structural design and analysis of floating bridges

Floating bridges have been used since ancient times, often in battles of war as temporary crossings. Technology and design concept has evolved a lot since ancient times, and in today's society, floating bridges are used permanently for traffic and civilian use. A floating bridge uses pontoons or other floating elements to support the bridge deck. The concept is from the natural law of buoyancy of the water, and the maximum load the pontoons can carry is limited to the buoyancy of the floating supports [19]. To maintain transverse and longitudinal alignments, anchoring and mooring lines or a structural system are needed. The vertical loads in the system are resisted by the buoyancy forces [19].

Figure 3.5 illustrates the two different types of pontoons a pontoon-supported floating bridge can have, where openings for marine traffic can be incorporated for both types:

- Continuous pontoon type, which are individual pontoons joined together and make a continuous structure [19].
- Separate pontoon type, which are individual pontoons placed separately transversely on the structure [19].

(a) Longitudinal continuous pontoons. Adapted from [19].

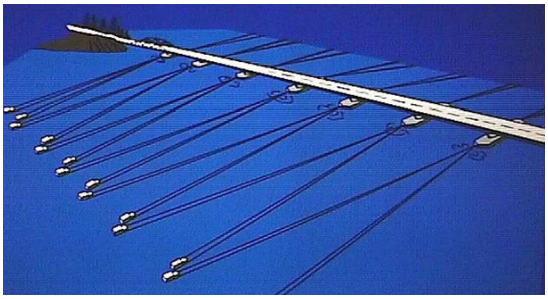

(b) Transverse separate pontoons. Adapted from [19].

Figure 3.5: Pontoon models for floating bridges.

3.2.1 Materials in Floaters

There are several different materials that can be used in floating bridges. The floating elements can be constructed in wood, steel and concrete, or in a combination of these materials [19]. As wood was a well-recognized material in the early stages of floating bridges, it is not a sustainable material to be used in floaters of modern floating bridges.

Steel pontoons will have high structural integrity [19]. One challenge with using steel in the floaters is the high cost of the material and unit weight of the steel. The use of steel in the floaters has been proposed in the project with Bjørnafjorden Bridge.

Modern floating bridges often consist of reinforced concrete (RC) pontoons. Concrete is relatively cheap compared with steel, and easy to access. The density of concrete is relatively low and is very light compared to steel properties. Highly corrosive resistant if the mix is right for the environment. In addition to good material qualities, concrete ensures good damping for vibrations and noise, and is less affected by fire and heat than steel [19].

To make the floaters as light as possible lightweight concrete (LWC) has been widely used for floating structures. The knowledge of the usage of lightweight concrete is from the offshore oil production development in Norway [37]. Several platform foundations were designed and constructed using LWC, like Troll B and Heidrun. The main purpose of using LWC is to reduce the weight of the structure. To be characterized as LWC the density has to be under 2000 kg/m^3. Constructions of LWC can have a more brittle behaviour than normal density concrete, but with the use of steel reinforcement, they will achieve the same structural ductility. The use of concrete in a marine environment requires decent durability of the concrete to withstand chloride-initiated corrosion of the reinforcement. Research shows that the lightweight aggregate in LWC is at least as durable as a concrete mix with normal density, as long as the binder content and quality are the same [37].

Prestressing of the reinforced concrete shows a good effect in strengthening the concrete structures according to research done by Sha and Amdahl in 2019 [27]. The numerical investigations indicate that prestressing ensures that the pontoon remains structurally intact throughout the entire collision process, preventing the formation of any holes in the concrete that could result in flooding [27]. In contrast, without prestressing, significant strains occur, leading to extensive damage around the perimeter of a simulated ship impact [27].

3.2.1.1 Fibre-reinforced Polymer

Fibre-reinforced polymer (FRP) is a composite material which combines polymers and fibres. It can be used as a material itself, or as a strengthening of the existing material

in the floaters. As demolishing and reconstructing existing structures is not economical when considering the cost, time and effort, FRP is an option to repair and strengthen the existing members [6]. It is relatively easy to transport, use and install. As it is already a common practice for strengthening concrete structures, it can also be used on other materials like steel and masonry [6]. The FRP-strengthening techniques can increase the collision capacity without increasing the dimensions of the members [29].

Fibre-reinforced polymers most often have fibres of glass, carbon or aramid. Carbon fibre reinforced polymers (CFRP) are mostly used in construction as a strengthening method as the properties of CFRP process best compared to steel properties, as shown in Figure 3.6 [6].

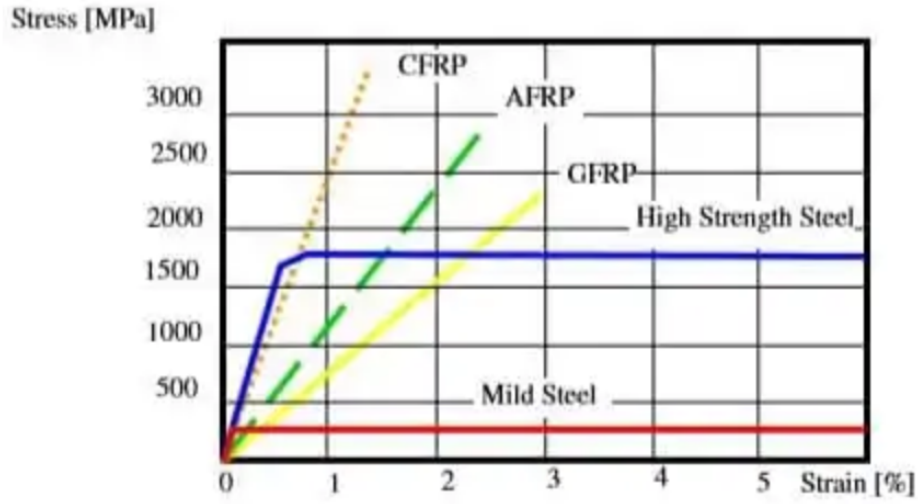

Figure 3.6: Properties of different FRP compared with steel. Adapted from[6].

The composite is light and strong, and has a high tensile strength and stiffness [6]. It reduces the brittleness as the ductility is improved and has a high resistance against ingress of unwanted substances [6]. In other words, the CFRP provides additional strength to reinforced concrete compared to glass and aramid fibres.

High cost is one of the primary disadvantages regarding fibre-reinforced polymers [6]. The production and implementation of FRPs can be expensive compared to traditional construction materials. Another significant concern is the recycling of FRPs, as the process can be challenging and complex [6]. Proper disposal and recycling methods for FRPs are still being developed and refined to ensure sustainability and minimize environmental

footprint.

3.2.2 Impact on Floaters

Floating structures are exposed to impact from environmental and service-related loads. A floating bridge must withstand dead loads and live loads from traffic. Environmental loads such as wind and waves will influence the marine structures, but currents, hydrostatic pressure and temperature will also play a significant role. In Norway, there is also important to consider tidal variations, marine growth, ice and snow on the deck of marine structures [38]. This can be a challenge when constructing floating bridges as strong currents, high wind speed and large waves can be demanding for the structural integrity [19]. Another challenge is the marine traffic. As the pontoons are floating on the sea surface, there can be limited opportunities to pass under the bridge for larger vessels.

Potential damages need to be considered when designing floating structures. The bridge needs to have the structural capacity to withstand collisions from vessels or other floating objects that may occur, flooding events, potential loss of mooring lines or components, as well as complete separation due to a fracture [19]. These considerations are crucial for ensuring the integrity and resilience of the floating bridge.

3.2.3 Accidental Limit State

An Accidental Limit State (ALS) is a condition where a structure reaches a condition where it no longer is suited for the intended function, or is no longer able to maintain its structural integrity as a consequence of accidental loads [7]. The intention of ALS design is to ensure that the structure can withstand specified accidental impact or avoid full collapse or other fatal situations after accidental load impact [7]. Accidental limit state evaluation is a key aspect of floating bridge design.

Examples of accidental loads can be vehicle collision, ship collision, falling objects, fire or explosion and in some cases extreme environmental loads such as earthquakes and flooding, dependent on the severity of the loads [7].

The current design codes employed for accidental loads, such as particularly ship collisions, are as follows:

- NS-EN 1991-1-7
- NORSOK N-004
- DNV-RP-C204
- AASHTO Guide Specifications and Commentary for vessel collision design of highway bridges for US design code

3.2.4 Ship Collisions with Floating Structures

Ship collision is one of the potential accidental loads a floating bridge should be designed for [19]. The ship collision action is characterised by kinetic energy, dependent on the mass of the vessel, including hydrodynamic added mass and the speed of the vessel at the point of impact [7]. There are several widely used design codes that govern ship collisions, which have become implemented in the maritime industry over the years. Notable examples include DNV-RP-C204, Eurocode like NS-EN 1991-1-7 and additionally, in Nordic countries, NORSOK N-004.

NORSOK N-003 specifies general principles and guidelines for the determination of characteristic actions and effects for the design, assessment and verification of structures [39]. It is applicable to offshore structures used in petroleum activities, including floating structures [39].

The NPRAs handbook N400 states that if the probability of accidental loads is less than 10e-4 per year it can be disregarded.

NS-EN 1991-1-7 states that the influence of impact load and choice of protection should be decided depending on the traffic on and under the bridge, and on the consequences of a collision [10]. The code specifies methods and guidelines to secure structures from known and unknown accidental actions. In Table 3.1 adapted from NS-EN 1991-1-7 some indicative values for impact forces due to ship collision in sea waterways are given [10].

Table 3.1: Table C.4 from NS-EN 1991-1-7 [10].

Table C.4 - Indicative values for the dynamic interaction forces due to ship impact for sea waterways.

Class of ship	Length ℓ= (m)	Mass m[a] (ton)	Force F_{dx}[b,c] (kN)	Force F_{dy}[b,c] (kN)
Small	50	3 000	30 000	15 000
Medium	100	10 000	80 000	40 000
Large	200	40 000	240 000	120 000
Very large	300	100 000	460 000	230 000

[a] The mass m in tons (1 ton = 1 000 kg) includes the total mass of the vessel, including the ship structure, the cargo and the fuel. It is often referred to as the displacement tonnage. It does not include the added hydraulic mass.

[b] The forces given correspond to a velocity of about 5,0 m/s. They include the effects of added hydraulic mass.

[c] Where relevant the effect of bulbs should be accounted for.

When investigating ship collisions there are several analysis approaches that can be used. The most common approaches are Finite Element Method, simplified analytical method, experimental method or empirical method [40].

Two mechanics are typically studied in ship collisions, external dynamics and internal mechanics. Internal mechanics involve analyzing how energy is distributed within the striking and struck parts during collisions [22]. This can be achieved through various methods such as full-scale collision tests, model tests, Nonlinear Finite Element Analysis (NFEA), or simplified analysis techniques [33]. The goal is to understand the dissipation of energy within the structures involved.

External dynamics analysis, on the other hand, focuses on the overall energy dissipation and is typically performed using time simulation procedures [22]. This analysis can be conducted using coupled or uncoupled approaches, utilizing classical mechanics principles [33]. The conservation of momentum and energy plays a significant role in understanding the dynamics of ship collisions and the subsequent dissipation of energy as strain energy [33].

According to NS-EN 1991-1-7, collisions can be classified into two categories: soft and hard impacts [10]. In the case of a hard impact, the major part of the energy from the impact

is absorbed by the vessel. A soft impact, on the other hand, refers to a scenario where the construction is specifically designed to absorb most of the impact energy through plastic deformations [10].

In Figure 3.7 adapted from DNV-RP-C204, there are three stages when considering the dissipation of energy by a collision: ductile design, strength design and shared-energy design [7].

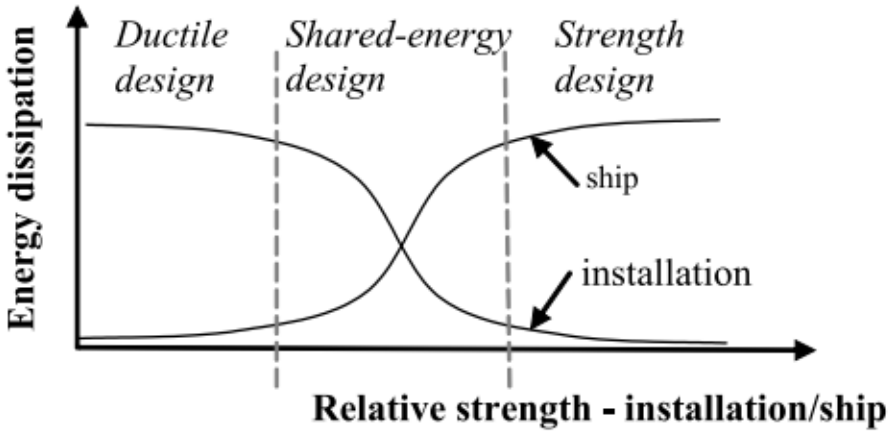

Figure 3.7: Energy dissipation for strength, ductile and shared-energy design from DNV-RP-C204 [7].

In strength design, the ship is engineered to dissipate the majority of the energy generated during an impact, while the installation experiences minor deformations compared to the ship [7]. This aligns with the characterization of a hard impact in Eurocode. On the other hand, ductility design presents the opposite condition, where the installation undergoes significant plastic deformation and contributes to the majority of the energy dissipation, while the ship experiences minimal deformation and energy absorption [7].

In the context of shared-energy design, both the ship and the installation are designed to dissipate a substantial portion of the impact energy. This results in significant plastic deformations for both entities involved[7].

The collision energy to be dissipated as strain energy for a fixed installation is given in equation 3.2 [7].

$$E = \frac{1}{2}(m_s + a_s)v_s^2 \tag{3.2}$$

Floating platforms may normally be considered as compliant according to DNV-RP-C204 [7], and the equation for the energy to be dissipated as strain energy is as follows:

$$E = \frac{1}{2}(m_s + a_s)v_s^2 \frac{(1 - \frac{v_i}{v_s})^2}{1 + \frac{m_s + a_s}{m_i + a_i}} \tag{3.3}$$

where:

m_s = mass of ship
a_s = added mass of ship
v_s = impact speed
v_i = velocity of installation
m_i = mass of installation
a_i = added mass of installation

The structural response of the system is represented as a relation between load and deformation, as seen in Figure 3.8 adapted from DNV-RP-C204 [7]. The strain energy dissipated in the collision, by the ship and installation, equals the total area beneath the load-deformation curve in Figure 3.8. The examination of collision mechanisms focuses particularly on the relationship between force and displacement during the impact. Understanding the force-displacement relation is of great interest when investigating the dynamics and behaviour of collisions [7].

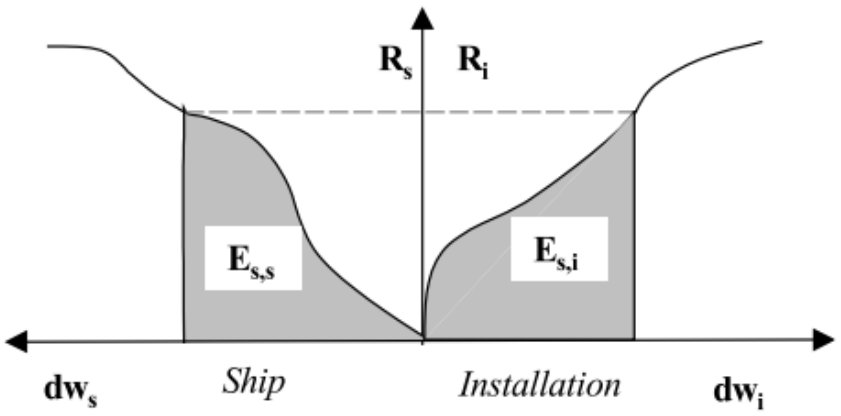

Figure 3.8: Dissipation of strain energy in ship and installation adapted from DNV-RP-C204 [7].

3.2.5 Failure Modes

Multiple failures are possible when constructions are exposed to accidental loads. In case of a ship-bridge collision, there will typically lead to large shear forces and bending moment resulting in damage or even collapse. Typical failure modes were evaluated from actual collisions between trucks and RC concrete piers by Buth et al. in 2010 [41]. In the experimentation, there were found that shear failure is most typical with high impact velocities in the accident[41].

For low impact velocities, which are more typical for ship collisions with a significant impact, there are more common with combined flexural-shear failures with flexural damages according to the research provided by Gholipour et al. [8]. Based on the observation from the experiment of Bush et al., an illustration of typical failures for an RC bridge pier under collision loads is adapted from Gholipour et al. in Figure 3.9 [8].

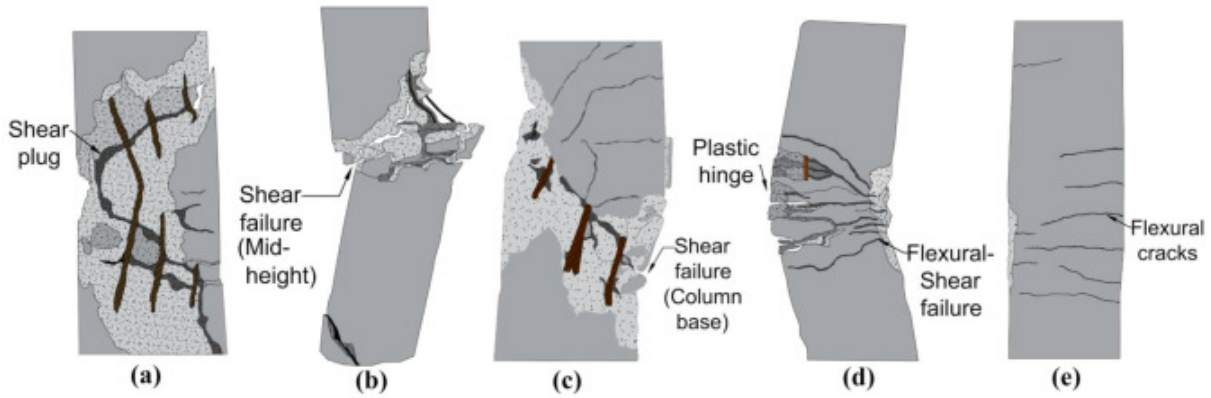

Figure 3.9: Typical failure modes for RC piers after impact loads. Adapted from [8].

3.2.6 Risk Assessment

To evaluate and identify the potential risks and hazards associated with ship collisions, a risk assessment can be performed. The aim of a risk assessment is to evaluate the probability and potential consequences of a collision between a vessel and the bridge structure. A risk assessment can address mitigation measures to reduce the risk of accidental loads and enhance the safety. Overall, conducting a risk assessment for ship-bridge collisions is a proactive approach aimed to improve the safety, avoid accidents and protect the environment and critical infrastructure. The key procedure in a risk assessment consists mainly of three steps [9]:

1. Evaluate the probability of ship collision
2. Estimate impact energy
3. Estimate structural damage to structures involved

The probability of the occurrence of collision can also be predicted from historical data, predictive calculations or experts' points of view [9].

The risk associated with a specific activity is defined as a function of the hazards, the probability of occurrence and all possible related consequences and can be presented as the following equation [9]:

$$Risk = f(hazards, probabilities, consequences) \tag{3.4}$$

$$Risk = SUM(P_i(H_i * C_i) * U_i(C_i)) \tag{3.5}$$

Where

C_i = the consequence related to the hazard
H_i = hazard
P_i = probability of the $_i$th consequence
U_i = utility function that expresses the consequence as the monetary value

To initiate a reliable risk analysis, the initial crucial step involves gathering information concerning the bridge's geometry, alignment, underwater terrain, road traffic, ship traffic, and environmental loads such as wind, waves, currents, and ice conditions [38]. Given that bridges typically are designed with a service life spanning over several decades, accurately forecasting of ship traffic over such a long period becomes a challenging task. Consequently, the risk analysis frequently focuses on a shorter time period to ensure practicality and feasibility [38].

The risk related to ship collision is dependent on the ship traffic in the sailing route and ship types. The intensity of the ship traffic is key information when predicting the probability of ship collisions. As the volume of ship traffic increases, it is anticipated that the frequency of accidents will rise correspondingly [9]. To predict ship traffic an Automatic Identification System (AIS) and radar data are important tools. AIS is mainly

an aid to reduce the possibilities for ship collisions, but is also used to give the government an overview of ship traffic. Ships over 300 tonnes are plotted by AIS history, while ships below 300 tonnes and navy vessels are collected by radar data [9]. In Figure 3.10, an example of the distribution of international ship traffic from satellite receivers is illustrated.

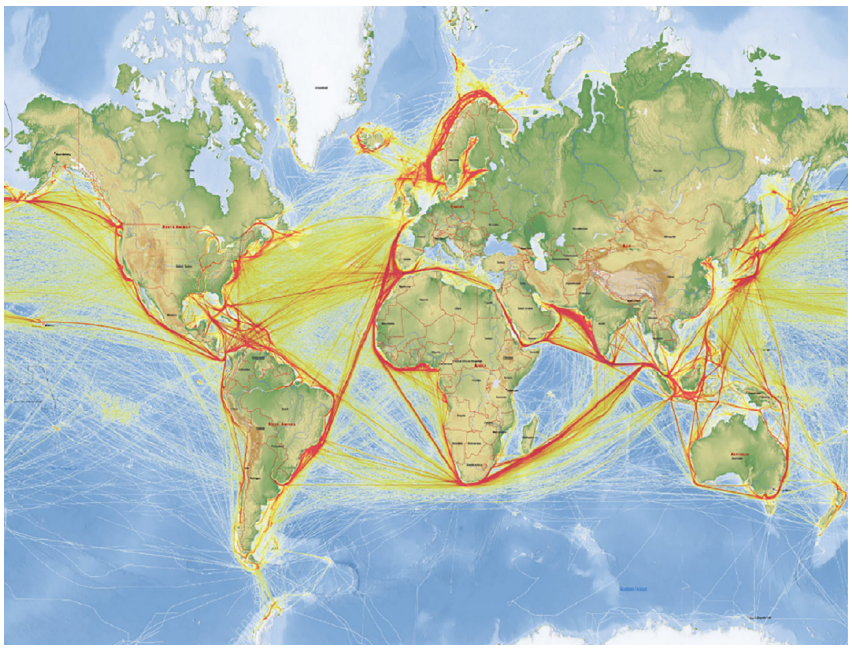

Figure 3.10: AIS tracking of ship traffic. Adapted from [9]

Four different risk categories are relevant for ship-bridge collisions [38]:

1. Human errors associated with ships following the ordinary straight route with normal speed
2. Ships that fail to make a proper change of the sailing course close to the bridge
3. Ships that do not follow the ordinary route that is recommended due to technical errors (mooring/anchoring failures, drifting ships due to work, loss of propulsion, steering gear failure)
4. Ships which make an evasive manoeuvre close to the bridge due to the presence of other vessels, and therefore collide with the bridge

Human errors are accounting for approximately 80% of all ship collisions, along with technical errors such as the loss of steering capacity and propulsion, which contribute to approximately 20% of all ship collisions [9]. It is important to note that the reporting of

these factors and the identification of error sources may be subject to under-reporting or potential errors in data collection of ship collisions.

The consequences of risk are usually divided into three main types of consequences [9]:

- Fatalities
- Pollution of the environment
- The loss of property or financial exposure

It is important to establish risk acceptance criteria for these main types of risk to find a balance between the safety and cost of achieving that risk level. In the context of bridge design, three distinct design philosophies are commonly employed: Deterministic design, Quantitative Risk Assessment and ALARP Cost Benefit Analysis [40].

In the approach of deterministic design, the bridge is designed to withstand impacts from the largest vessel expected to operate in the area, without considering the probability of such impacts actually occurring [40].

A quantitative risk assessment is a design philosophy where the bridge is designed to achieve a specified level of risk, considering the probability of failure due to ship collisions without considering the associated cost [9].

ALARP Cost Benefit Analysis where ALARP stands for "As Low As Reasonably Practicable", involves designing the bridge to achieve a risk level that is economically optimal. This approach balances the costs associated with reducing the risk against the potential benefits gained from risk reduction measures [9].

3.2.7 Risk Minimizing Measures

When dealing with high-risk impacts, it is crucial to implement effective risk-minimizing measures to mitigate potential consequences. These measures intend to reduce the probability of accidents or minimize the severity of the impacts. Reducing the probability of ship collisions is recognized as the most cost-effective approach to mitigating risks [42]. Numerous tools and strategies can be employed to effectively minimize the likelihood of such incidents. In NS-EN 1991-1-7 a general description of different strategies for accidental design situations is given, and is presented in Figure 3.11 [10].

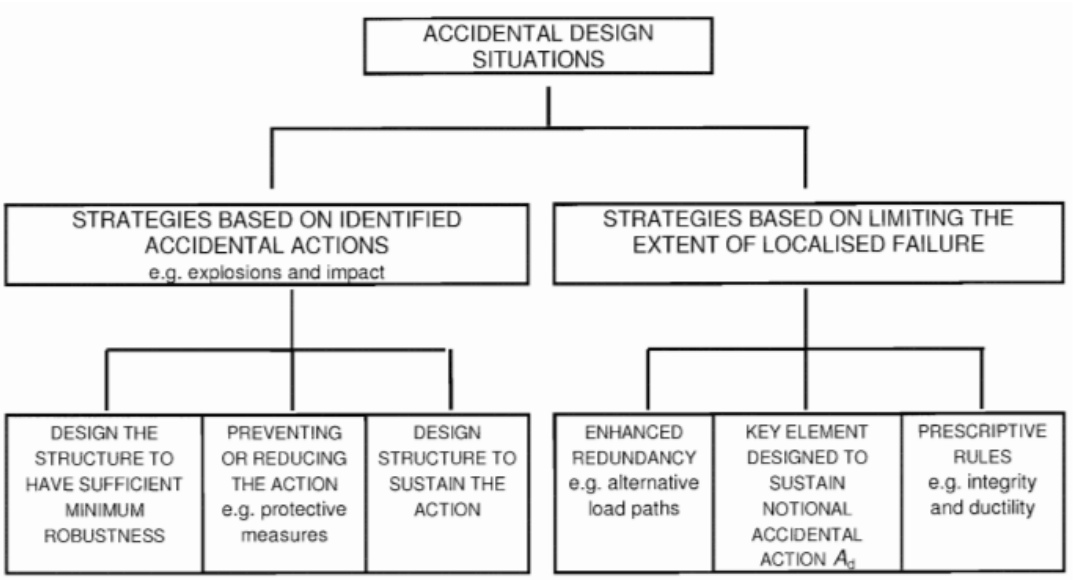

Figure 3.11: Strategies for Accidental Design Situations. Adapted from NS-EN 1991-1-7 [10].

The Vessel Traffic Service (VTS) is an international service to provide navigational advice and protection of the environment and ensures safe passage for vessels [43]. In Norway, the VTS is operated by the Norwegian Coastal Administration and is recognised as a risk-preventing measure as the VTS service monitors and informs vessels about maritime traffic to avoid unwanted situations in areas associated with risk. Provide the service on various sources such as AIS and radar sensors [43]. In the study of the probability of ship collisions by Zhang et al., it revealed that the inclusion of a VTS system can potentially decrease the likelihood of ship-bridge collisions by a factor of 2-3 [9]. Similarly, the presence of a pilot on board is frequently simulated to reduce the causation factor to approximately half or one-third of the original probability [9].

Another measure that has been recognized as a useful way to reduce ship collisions is different warning systems such as Collision alert systems (CAS) and collision prevention systems [44]. Conservative design of installations in areas exposed to maritime traffic is crucial, as repair and replacement often are difficult and not cost-effective compared to other measures to reduce the risk for collapse.

The navigational channel layout of bridges is one of the parameters to consider when reducing the probability of ship collisions. It is often necessary to improve the layout of the navigational channel, giving the channel a direction close to perpendicular to the bridge.

A navigational channel perpendicular to the bridge direction gives a better overview and reduces the need of changing course before crossing beneath the bridge [9].

4 Nordhordland Bridge

A description of the specific design of Nordhordland Bridge will be given in this part of the thesis. The ship traffic in the area will be plotted and the probability of ship collisions to the bridge will be investigated.

4.1 Nordhordland Bridge

Nordhordland Bridge is a curved floating bridge, with a radius of 1700 m. The curved design will transfer the shear forces to the land connection at the ends of the bridge. This bridge is one of two specimens in Norway, as it is constructed similarly to Bergsøysund Bridge, which opened in 1992. The pontoons on Nordhordland Bridge are floating freely without any lateral moorings and anchors lines on the sides. This is because of limitations due to the great depth in Salhusfjorden, which is about 500 m where the bridge crosses the fjord [12]. The floating part is therefore connected with shore anchorage at the ends. Different views of the bridge are given in Figure 4.1 and 4.2.

As mentioned in the introduction NS 3472 for steel structures, NS 3474 for concrete structures and NPRA´s Handbook 185 were used as design codes for the bridge. The owner of the bridge is the Norwegian Public Roads Administration, and the structural designers were Dr. ing A.Aas-Jakobsen AS and Det Norske Veritas Industry AS. Design control was conducted by Consulting Eng. A.R Reinertsen, and Veidekke, Norwegian Contractors and Kværner Eureka were the ones building the bridge [37].

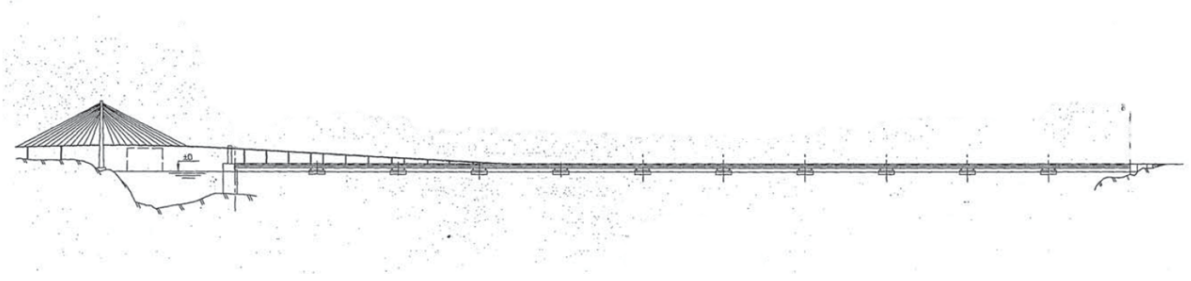

Figure 4.1: Side elevation of Nordhordland Bridge [11]

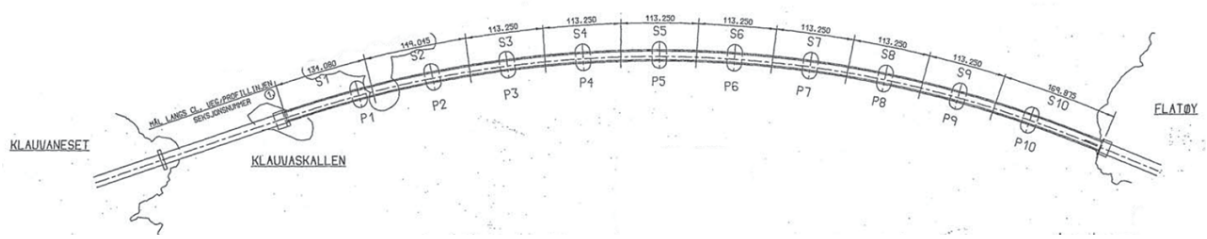

Figure 4.2: Plan view of Nordhordland Bridge [11]

4.1.1 Bridge Girder

The bridge girder is a steel box girder as shown in Figure 4.3, and is the most important element of the bridge system. The girder has to withstand large forces transferred from the supports on the pontoons and pillars of the viaduct [12]. The steel box girder is placed on top of the floating part of the bridge all the way from the shore at Flatøy and to the fixed deep water foundation. The carriageway is placed on top of the box girder and continues on pillars by the viaduct up to the high-level bridge.

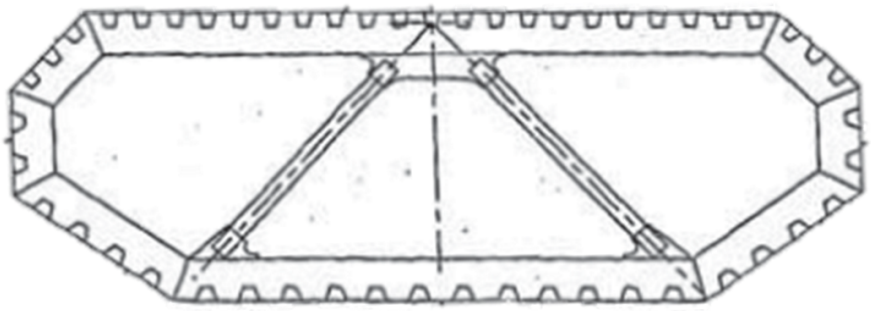

Figure 4.3: Nordhordland Bridge cross-section of the bridge girder [11].

The height of the carriageway varies in the range from 11 to 34,4 m above sea level. This led to one of the greatest challenges to identify: how to connect the viaduct to the floating part of the bridge with tidal movements and how to connect the shore anchorage, without transferring unacceptable high forces from the floating bridge over to the viaduct [12]. The solution was specially designed flexible plates in the connection to the shore anchorage. The flexible plates allow deformations due to the tidal movements in the floating bridge, and will also transfer the vertical-axis bending moment, axial forces and horizontal shear

forces from the bridge girder to the shore [12].

Steel with a yield strength of a minimum of 540 MPa is used from the shore anchorage at Flatøy and past the first of the pontoons, due to large variation in tension along the bridge. There are used normalized steel with a yield strength of 355 MPa on the remaining part of the bridge [12].

The distance between the underside of the box girder and sea level is 5,5 m, which allows small boats to pass under the floating part of the bridge in addition to the navigational channel.

4.1.2 The High-level Bridge

The high-level part of the bridge is a cable-stayed bridge and has a length of 369 m. The cables supporting the structure are attached to the tower with a height of 99.3 m. This design provided the best solution for ship traffic, giving a maximum sailing height of the navigational channel [12]. The high bridge provides a navigational channel for vessels with a height of 32 m and a width of 50 m. The high bridge is resting on a fixed deep water foundation on an underwater ridge at a depth of 30 m and is connected with shore anchorage. Figure 4.4 illustrates the fixed deep water foundation. The floating part and the cable-stayed part of the bridge are not structurally linked [45]. This means that the cable-stayed part is independent of the structural integrity of the deep water foundation, and would be able to carry itself if the fixed deep water foundation was disconnected.

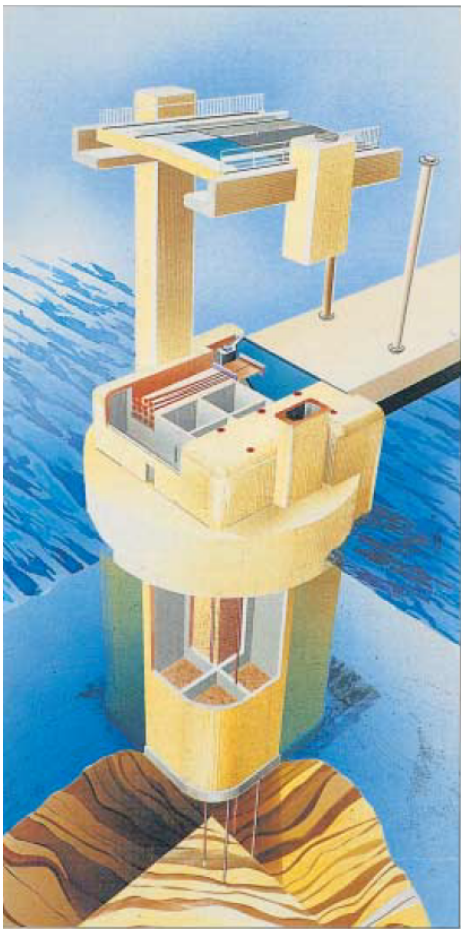

Figure 4.4: Illustration of the fixed foundation. Adapted from the NPRA [12].

The main span of the high bridge is constructed in LC55 light-weight concrete with a density of 1893 kg/m^3 to maintain the lowest possible weight. The cable tower is cast in standard C45 concrete and has a typical H-form [12].

Major forces are kept under control with the 48 cables
stretching from the tower. The capacity strength of the cables ranges from 1,96 kN to 7910 kN, depending on the distance from the tower [12].

4.1.3 Pontoons

The floating bridge consists of 10 prestressed RC pontoons, and they are the main parts to be analysed in this paper. The bridge has a separate pontoon type and they make the foundation of the floating bridge. An illustration of the pontoon and the connection to the rest of the bridge is given in Figure 4.5. The pontoons were built near Fredrikstad in Norway in a dry dock and later floated to their final location in Salhusfjord [37].

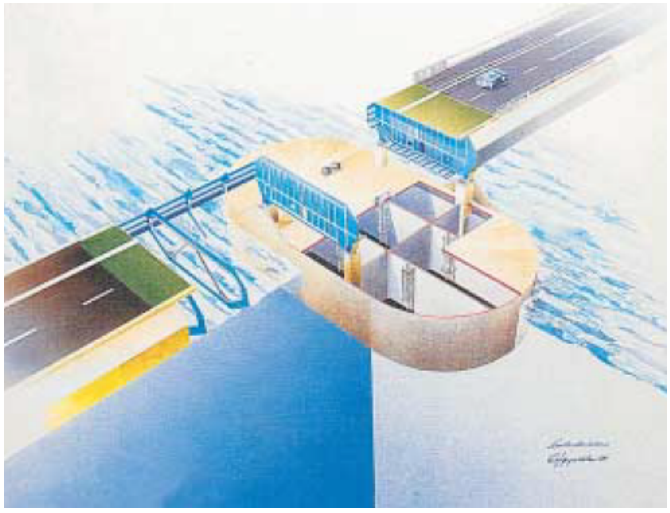

Figure 4.5: Illustration of the pontoons at the bridge. Adapted from the NPRA [12].

The dimension of the pontoons is 42 x 20.5 x 7.2 m, as shown in Figure 4.6. The two pontoons in the ends, on the other hand, have a height of 8.9 m. The outer concrete walls of the pontoons are 310 mm thick. The theoretical span between each of the pontoons is 113,25, and the draught varies depending on if the pontoon is near the shore or placed in the middle of the fjord [12]. The pontoons are divided into 9 cells/compartments. They are designed to avoid any endangering to the bridge even if 2 neighbouring cells out of the total 9 cells are filled with water due to large damages after impacts etc [12].

The material of the pontoons is lightweight concrete, LC55. The material is chosen considering the durability and weight of the structures. Lightweight concrete LC55 receipt for the pontoons is given in Table 4.1 [37]:

Table 4.1: Composition of lightweight concrete mixture, LC55

Density	1950 kg/m^3
Compressive strength	55 MPa
Cement CEM 1	410 kg/m^3
Microsilica	33 kg/m^3
Sand 0-5 mm	675 kg/m^3
Liapor 8 4-8 mm	270 kg/m^3
Liapor 8 4-16 mm	325 kg/m^3
Water	200 kg/m^3
Retarder	0 - 0.3 l
WRA	2 - 3.5 l
HR WRA	6 - 7.5 l
AEA	0.05 - 0.15 l

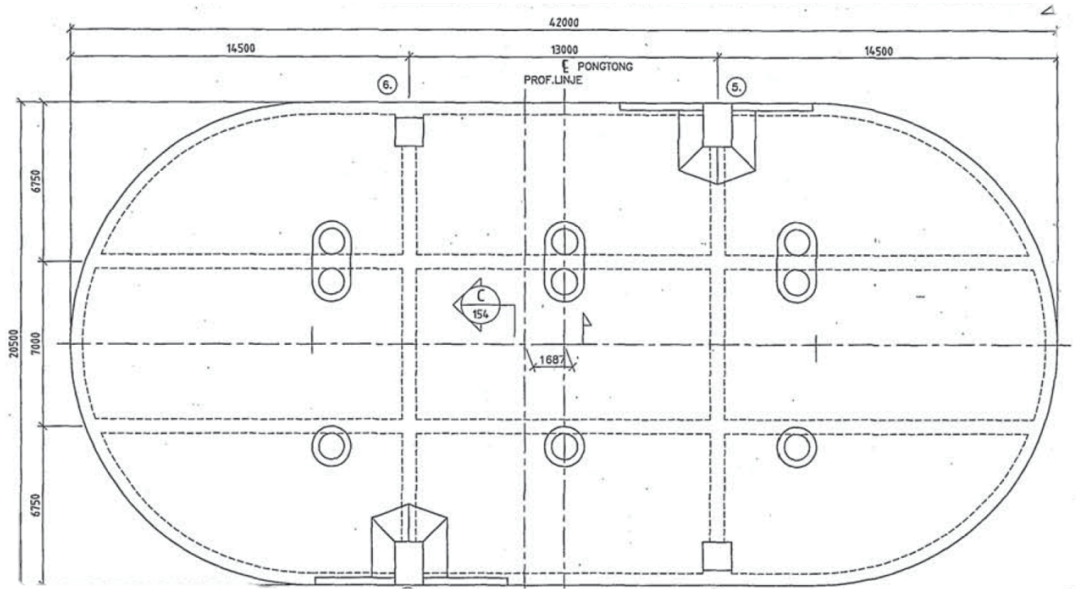

Figure 4.6: Plan view of pontoon [11].

The pontoons are subjected to various loads: permanent dead load from steel box girder and carriageway, traffic loads, environmental loads, buoyancy, drag forces, and thrust. They follow the motion of the sea during the change in water level, and there are significant tidal effects on pontoon number 1, 2 and 3 counted from the deep water foundation at the end of Klauvaneset. The largest tidal effect is on the pontoon closest to the fixed foundation, and then it gradually decreases and gets negligible after the third pontoon [12].

In the calculation of the design load from the initial design of Nordhordland Bridge, there is stated that the RC pontoons were designed to withstand an impact energy of 25 MJ

[45]. Only the first 5 pontoons from the fixed deep water foundation were considered under the calculations, but as the design is roughly the same for all 10 pontoons, it is assumed that they all have equal capacity [45]. As the floating and the cable-stayed part are not considered structurally linked, the separate calculations done in the design stage of the bridge may have contributed to a larger probability for collapse than expected [45].

4.2 Ship collisions that have occurred

As mentioned in the introduction of the thesis, there have been several ship impacts with the two floating bridges in Norway, Nordhordland- and Bergsøysund Bridge, during their lifetime. Three collisions of significant matter have been reported, two at Nordhordland Bridge and one at Bergsøysund Bridge.

4.2.1 Bergsøysund Bridge 2023

In March 2023 the first reported ship collisions occurred at Bergsøysund Bridge. The cargo vessel Tornado hit one of the floating pontoons at Bergsøysund Bridge due to incorrect navigation. As the crew discovered the deviation from the fairway approx. 100 meters before colliding with the bridge, they were able to reduce the velocity to 6-8 knots [13]. The impact was a typical glancing blow towards the pontoon, where the ship bow did not directly hit the concrete wall in the pontoon. Further on the vessel hit the steel girder of the bridge with the front hull of the ship. The diagonal steel girders took most of the impact. Inspections were performed after the impact. Some small insignificant damages were detected on the top surface of the pontoon, and some more severe deflection on the steel girders. No larger damages were found on the pontoons as seen in Figure 4.7b, so no need for repair in the concrete at the time when this thesis was written [13].

(a) Vessel Tornado after collision

(b) RC pontoon after collision

Figure 4.7: Ship collision at Bergsøysund bridge in 2023 [13]

Bergsøysund Bridge has no navigational channel under the bridge, so it allows only small boats to cross beneath. This is normally not a problem as the fjord crossing is not a part of the fairway for larger vessels. The results of these actions show that there is still a possibility to have ship collisions with larger vessels at Bergsøysund Bridge.

Table 4.2: Properties of Tornado [16].

TORNADO	
Ship type	General Cargo
IMO	7042291
Length overall (LOA)	50 m
Deadweight tonnage (DWT)	593 t
Gross tonnage (GT)	712 t
Max Speed / Average speed	11 kn / 8.5 kn

A simplified estimation of the static impact load of a stiff structure is proposed in equation 4.1 and the impact energy in equation 4.2 [45].

$$Impact\ Force\ P = 0.5 \times {W_d}^{0.5} \tag{4.1}$$

$$Impact\ Energy\ E = 0.5 \times (m + m_a) \times v^2 \tag{4.2}$$

where:

W_d = ship in dead weight tons (DWT)
m = mass of ship ($1.33 \times DWT$)
m_a = added mass
v = impact speed

Assuming 20% added mass for a head-on impact and a velocity of 8.5 knots, the impact from Tornado on Bergsøysund Bridge can be estimated by considering the data given in Table 4.2:

$$Impact\ Force\ P = 0.5 \times 539^{0.5} = 11.6MN \tag{4.3}$$

$$Impact\ Energy\ E = 0.5 \times (1.2 \times 1.33 \times 539) \times 4.4^2 = 8.3MJ \tag{4.4}$$

4.2.2 Nordhordland Bridge 2019

In June 2019 there was a ship collision with the cargo vessel, Framfjord, and Nordhordland Bridge. The damages on the bridge after the impact were stated to reduce the fatigue life of the steel structures, and the total cost of the repairs was approx. 9 million. In the impact, there was only the steel box girder that was damaged and not any of the floating concrete pontoons of the bridge. This ship collision most likely happen due to a human error, where the chief mate may have fallen to sleep or have acted negligently, and the ship missed the navigational channel beneath the bridge. The ship took most of the energy from the collision and got so large damage that it was scraped after the impact [14].

Table 4.3: Properties of Framfjord [17].

FRAMFJORD	
Ship type	General Cargo
IMO	8913473
Length overall (LOA)	80 m
Deadweight tonnage (DWT)	1688 t
Gross tonnage (GT)	1508 t
Max Speed / Average speed	10 kn / 9.2 kn

Figure 4.8: Ship Collision at Nordhordland Bridge in 2019 [14]

Assuming 20% added mass for a head-on impact and average speed, the impact from Framfjord on Nordhordland Bridge can be estimated by considering the data given in Table 4.3:

$$Impact\ Force\ P = 0.5 \times 1688^{0.5} = 20.5MN \tag{4.5}$$

$$Impact\ Energy\ E = 0.5 \times (1.2 \times 1.33 \times 1688) \times 4.73^2 = 30.1MJ \tag{4.6}$$

4.2.3 Nordhordland Bridge 2009

The first ship impact on Nordhordland Bridge happened in June 2009, when the cargo vessel, Nyfjell, hit the fixed deep water foundation of the bridge. The incident was caused by human error in the form of acute illness right before passing the navigational channel [46]. After the impact, half a cubic of concrete was lost from the deep water foundation of the bridge. Neither in this impact, did the pontoons got hit or damaged.

Table 4.4: Properties of Nyfjell [18].

NYFJELL	
Ship type	General Cargo
IMO	7602584
Length overall (LOA)	67 m
Deadweight tonnage (DWT)	1321 t
Gross tonnage (GT)	1155 t
Max Speed / Average speed	10 kn / 8.5 kn

Figure 4.9: Ship Collision at Nordhordland Bridge in 2009 [15].

Assuming the ship held an average speed of 8.5 knots during the impact and a 20% added mass for a head-on impact, a simple estimation of impact load and the impact energy can be calculated by considering the data given in Table 4.4:

$$Impact\ Force\ P = 0.5 \times 1321^{0.5} = 18.2MN \tag{4.7}$$

$$Impact\ Energy\ E = 0.5 \times (1.2 \times 1.33 \times 1321) \times 4.37^2 = 20.1MJ \tag{4.8}$$

To summarise, despite the ship collisions that have occurred on the two floating bridges in Norway, no one has so far led to catastrophic consequences in the form of loss of human life or fatal structural damages to the bridge structure. The bridges were not taken out of commission after the collisions, so the collisions only affected the economic aspects in the form of repairs [45]. This despite that from simple calculations seems like the impact energy from the collisions has been in the range of the design load of 25 MJ. It is important to state that the impact energy calculated is just a simplified approximation. Many parameters have an estimated value, as the exact speed in the moment of collision is uncertain, and this affects the impact energy calculated.

4.3 Local Ship Traffic

The navigational channel beneath the High-level bridge allows larger ships to pass at the end of Klauaneset, while smaller boats can also pass under the steel box girders of the floating part of Nordhordland bridge. There is mostly local ship traffic where most of it is cargo vessels and smaller passenger ships passing in the area, but as it is one of the main passages into the port of Bergen city, there is a possibility for larger ships to pass and this must be considered. The Norwegian tourist cruise, Hurtigruten, is sometimes using this route when entering the port of Bergen.

To analyse the local ship traffic, historical data from 2015 and 2016 from AIS of vessels over LOA 25 m plotted in Figure 4.10 plotted by NPRA in a risk analysis of the Nordhordland Bridge done in 2017 [3]. Ships with LOA less than 25 m have been excluded in this study to get a more precise traffic model for the relevant traffic when considering accidental loads [3].

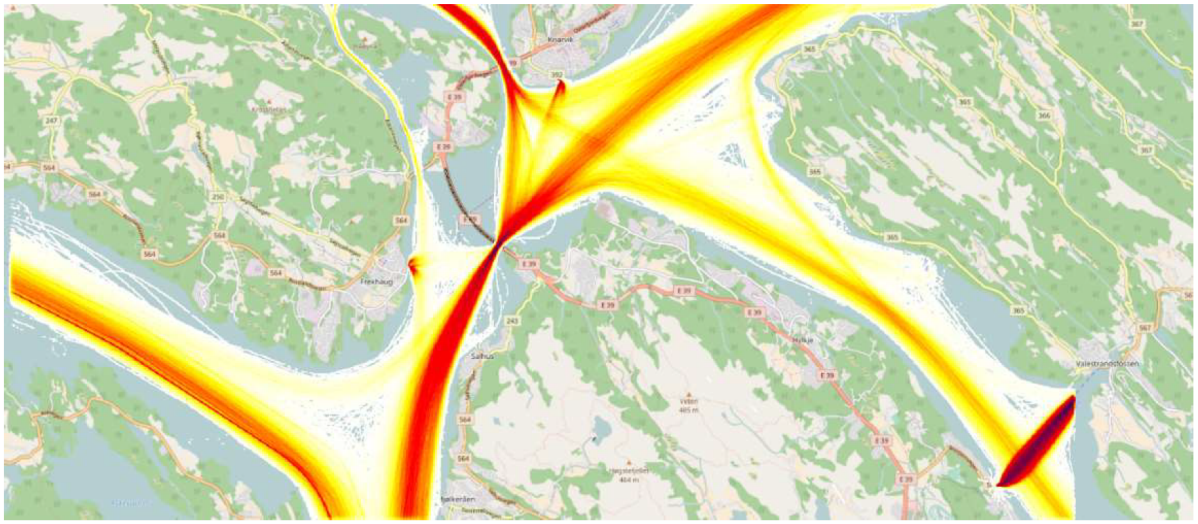

Figure 4.10: Ship Traffic of vessels LOA > 25 m from 2015 to 2016 [3].

From the risk analysis performed by the NPRA, there where found that [3]:

Annual frequency of ships in the area from AIS < 100m: 5417 vessels

Annual frequency of ships in the area from AIS > 100m: 328 vessels

This indicates a decent passage of ships beneath the bridge.

4.4 Probability of Ship Impact at Nordhordland Bridge

Two potentially severe collisions have already happened at Nordhordland Bridge, and as there still occurs ship traffic in the area of the bridge, it poses a risk for several ship collisions. It is very important to address the potential risk and probability of ship collisions in order to prevent possible ship impacts with tragic outcomes. The Norwegian Coastal Administration forecasts that the ship traffic will increase by 19% in the Norwegian fjords from 2018 to 2050, and predict growth in most of the ship classes, especially cargo vessels [20].

NS 3472 (now NS-EN 1993) for steel structures and NS 3474 (now NS-EN 1992) for concrete structures together with NPRAs Handbook 185 was used to design Nordhordland Bridge together with NPRA's Handbook 185 [45]. The NS design codes used during the design of the bridge in the 1990s do not seem to include specific requirements or guidelines regarding impact loads from ships. NPRAs handbook 185 on the other hand, stated that if the probability of accidental loads is less than $10e^{-4}$, it can be disregarded

when designing the bridge [45]. The requirement in the codes for bridge design by today are more consistent, and bridges are required designed after a probability of 10^{-4} for accidental impacts [10].

The NPRA has, as mentioned earlier, performed a risk analysis of the bridge in 2017 [3]. Two years of ship traffic data from AIS were utilized in the analysis calculating the probability of ship impact along the different parts of the bridge using the software IWRAP [3]. An intensity plot from the analysis shows the probability of ship collisions in the different parts of the bridge:

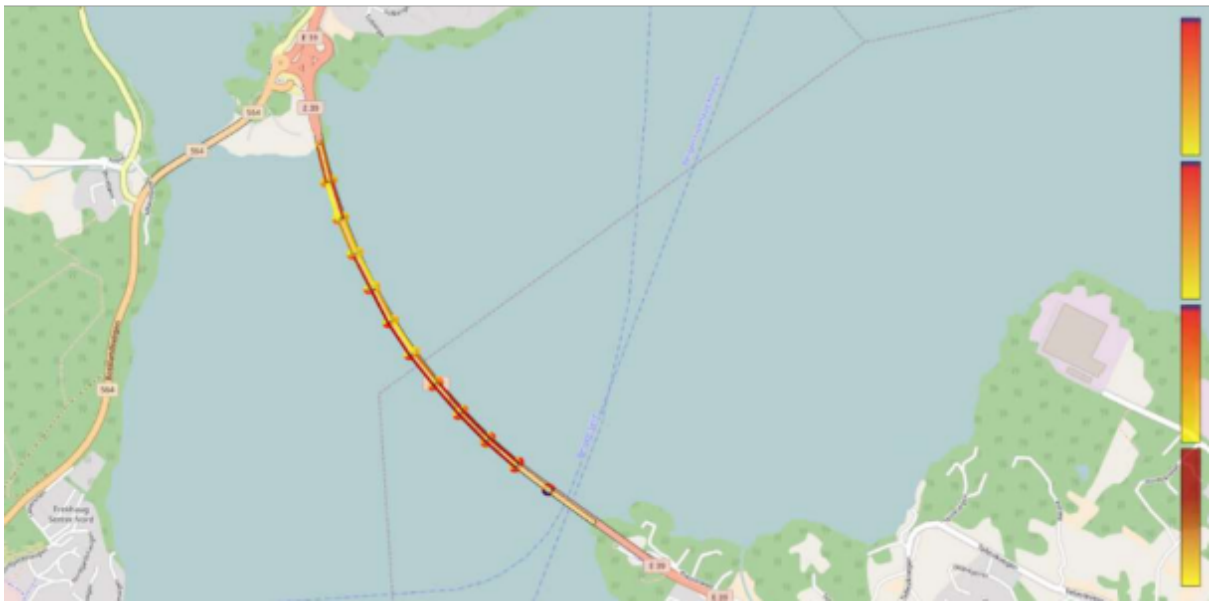

Figure 4.11: Probability for ship collision to the different parts of Nordhordland Bridge [3]

Figure 4.11 shows that the probability for ship collisions at the pontoons is largest at the pontoons closest to the navigational channel, but there is still a significant risk for the rest of the pontoons as well.

From Mathias Egeland Eidem's research done in 2022 [45], a simple probability analysis is proposed. An estimate of the probability for a ship impact from a ship with LOA $<$ 100 m is found with the formula provided by Eidem, based on that there have been 2 ship collisions on Nordhordland Bridge during a service life of 28 years [45]:

$$P_{collision} = \frac{Number\ of\ Impacts \times Critical\ length}{Number\ of\ years \times Total\ length} \tag{4.9}$$

The probability analysis assumes an impact against the critical area of the pontoons, which will give a critical length of 100 m, as the 10 pontoons have a width of approximately 10 m [45]. The result of the analysis conducted is significantly over the requirement for considering accidental impacts, and are given in the following equations[45]:

$$P_{collision}(LOA < 100m) = 5.6e^{-3} \tag{4.10}$$

$$P_{collision}(LOA > 100m) = 3.4e^{-4} \tag{4.11}$$

This analysis is based on a simplified formula with an estimation of the probability of ship impact with Nordhordland Bridge, and can only be used as an indication of the probability of ship collisions. The annual frequency of ship traffic used in the analysis is from 2017, and there is expected to be more frequent ship traffic in the last six years, so this affects the accuracy of the probability.

To summarise, the risk analysis performed by Eidem [45] and from NPRA [3], indicates that the probability of ship collision at Nordhordland Bridge is larger than the requirement of $10e^{-4}$ in the code, and the probability for accidental impacts from all vessel with LOA over 25 m not be neglected. There is therefore important to determine the capacity of the bridge as it is today, as there is a possibility of ship collision to consider. As the Norwegian Coastal Administration expect growth in ship traffic over the next 25 years, the probability of ship collision will neither reduce in the coming years [20].

5 Local Ship-Pontoon Collision Analysis

In this chapter, the local nonlinear dynamic collision analysis and the process of achieving a representative finite element model of the concrete pontoon and ship in LS-DYNA will be described. The analysis approach used for this thesis is a numerical analysis to run a realistic representation of a ship-bridge collision at the pontoons at Nordhordland Bridge. The purpose is to investigate the structural capacity of the concrete pontoons after a ship collision. Several impact scenarios will be evaluated in the analysis. The simulation is s integrated ship-bridge collision, where a deformable ship hits a deformable pontoon.

5.1 Various Impact Scenarios

Several different impact scenarios will be looked into to identify the threshold at which the concrete pontoons will sustain significant structural damages, compromising the overall integrity.

5.1.1 Impact Angle and Position

Three different impact scenarios will be investigated in the analysis, and is illustrated in Figure 5.1:

- Head on impact in the centre of the pontoon (0°).
- Head on impact off the centre of the pontoon, straight towards the inner concrete wall of one of the cells inside the pontoon (0°).
- Glancing blow of the pontoon, where the ship will slide against the side of the pontoon (35°).

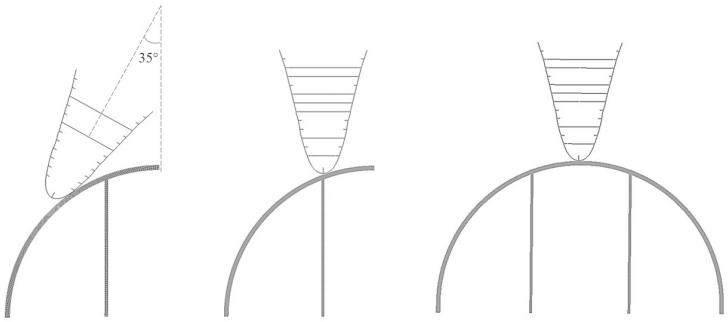

Figure 5.1: Impact scenarios

5.1.2 CFRP Strengthening Method

In an effort to enhance the strength of the concrete walls, the application of a protective layer of CFRP will be considered for the pontoon model. The objective is to increase the capacity of the pontoon to withstand the substantial impact energy resulting from a 2000-ton displacement ship collision. This approach is particularly intriguing for potential rehabilitation of the pontoons to ensure increased safety margins. By incorporating a model of the CFRP, the aim is to compare the capacity of the RC pontoon with and without a protective layer. Two methods of using CFRP are analysed, where thickness, fibre orientation and arrangement of the sheet are different.

5.2 Finite Element Analysis in LS-DYNA

The analysis involves three finite element (FE) models: an RC pontoon model, a ship bow model and a CFRP model. The FE modelling process can be summarized briefly as follows:

- Modelling of geometry and meshing
- Provide the geometry material and sections
- Acquire relevant properties to the model, such as contact, constraints, boundaries and impact.
- Run simulation
- Evaluate the results

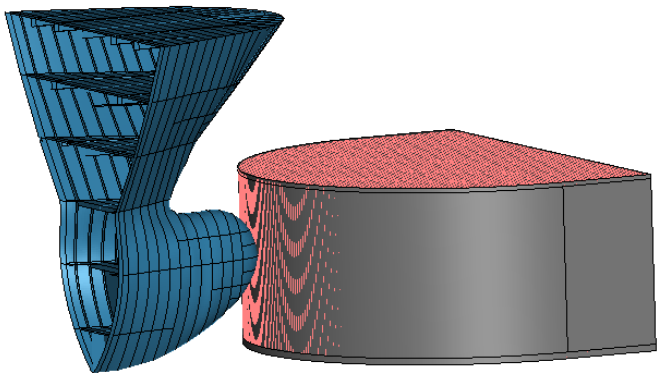

Figure 5.2: Overview of FE model

Considering the dynamic nature of the collision with a short-duration load application, an explicit analysis using LS-DYNA will be conducted. To accommodate the substantial computational resources needed for the analysis, the simulations will be executed on a High-Performance Computing (HPC) Fram, situated in Tromsø, provided by Sigma2- the National Infrastructure for HPC and Data Storage in Norway. Remote access to the HPC Fram will be established using the Bitwise SSH Client.

5.3 Pontoon Model

The FE model of the pontoon is modelled as a solid part, using under-integrated solids elements. The measures are followed from the original construction drawings from the NRPA with a height of 7.2 m and a thickness of 310 mm on the concrete wall in the area of impact. The solid elements are given a stiffness-based hourglass control with the keyword HOURGLASS to stabilise the elements as described in Chapter 3.1.2. The hourglass coefficient is set as 0.05 to set a low value in order to minimize the occurrence of non-physical stiffening in the system's response. However, it is still able to effectively suppress the development of zero-energy modes. The material model used for the concrete in the solid parts in LS-DYNA is MAT_CSCM. The material model properties included in the simulation are given in Table 5.1.

To allow failure and erosion in the material model, the keyword MAT_ADD_EROSION is added. This will provide the possibility to consider failure and erosion in the material of the concrete pontoon [47].

The pontoon model is modelled with two layers of longitudinal and transverse steel reinforcement with a diameter of 16 mm and 150 mm from centre to centre. The rebars are Hughes-Liu beam elements, which is the default beam formulation in LS-DYNA. The material model MAT_PIECEWISE_LINEAR_PLASTICITY is used for the steel reinforcement. This material model will define an isotropic elasto-plastic material which can undergo plastic deformation [34]. As the reinforcement was placed after the pontoon model was created, the nodes of the rebars and concrete elements did not line up and merge at all points. To connect the rebars to the concrete, the keyword LAGRANGE_IN_SOLID is used to constrain the reinforcement to the concrete elements in the pontoon model. It couples the rebars as the slave part and the concrete as the master part. An illustration

of the concrete pontoon model with reinforcement is shown in Figure 5.3.

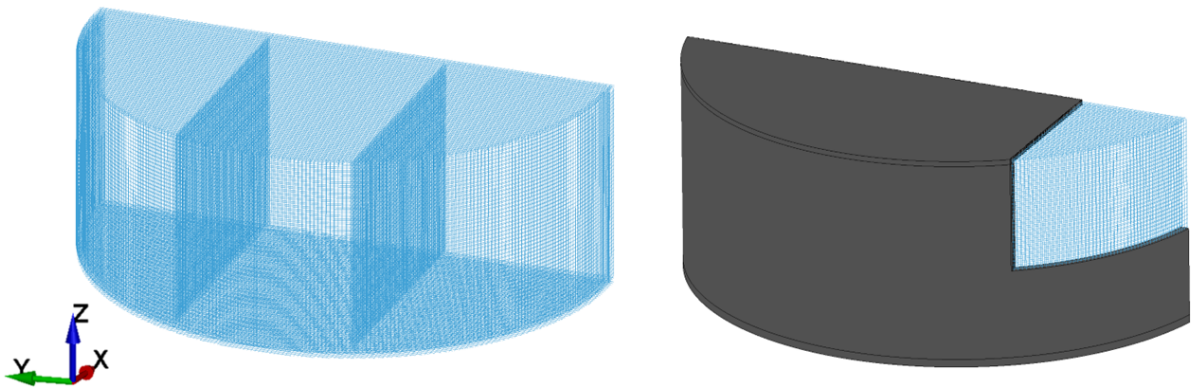

Figure 5.3: RC Pontoon Model in LS-DYNA

The pontoon model is modelled with a detailed, fine mesh. The provided mesh are giving elements of a size of approximately 50x50 mm all over the surface (Fig 5.4b). As the pontoon model consists of several parts connected together, a continuous mesh is hard to achieve under discretization.

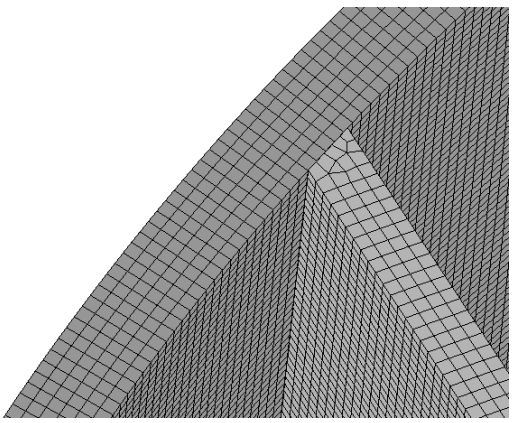

(a) Contact algorithm used to ensure contact between the parts.

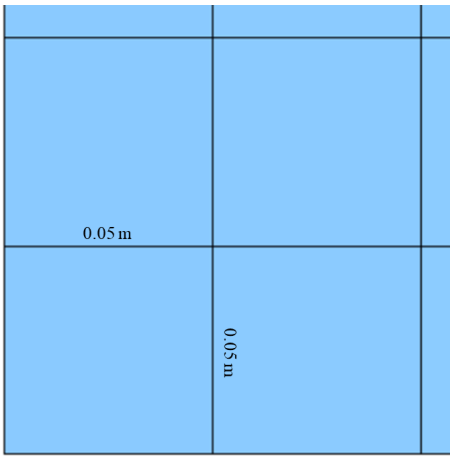

(b) Mesh size of the pontoon model.

Figure 5.4: Mesh of Pontoon model.

To solve the problem with noncontinuous mesh across the different parts of the pontoon model, as seen in Figure 5.4a and 5.5, the contact keyword TIED_NODES_TO_SURFACE is applied to tide the nodes together where the mesh is incoherent.

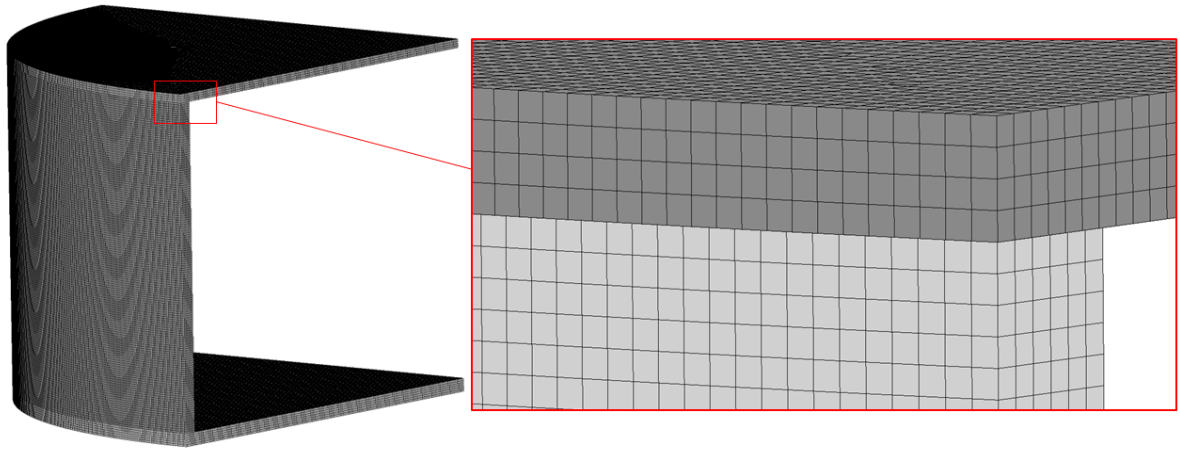

Figure 5.5: Incoherent mesh in pontoon model

The geometry of the pontoon model is based on the drawings of the pontoons represented in Chapter 5, with some simplifications of the design. As most of the structure is far from the impact region, the results are not expected to be affected by the simplifications done. Based on these assumptions a reduction in the FE model of the pontoon is conducted. Only half the pontoon was modelled to save computational resources, and in some of the simulations, even more, sections of the pontoon are removed to reduce computing resources and costs due to a large model with a fine mesh.

Table 5.1: Material parameters for RC Pontoon Model in LS-DYNA

Material	Material Model	Properties	
Concrete	MAT_CSCM	Density	1950 kg/m^2
		Poisson's ratio	0.2
		Compressive strength	55 MPa
		Shear Modulus	14.4 GPa
	MAT_ADD_EROSION	Failure strain	0.1
Steel Reinforcement	MAT_PIECEWISE_LINEAR_PLASTICITY	Density	7800 kg/m^2
		Poisson's ratio	0.3
		Yield stress	588 MPa
		Young's modulus	200 GPa

5.4 Ship Bow Model

The ship bow model of a container ship with mesh and material models was provided by associate Prof. Yanyan, supervisor of the project, from previous research (Figure 5.6). The FE model of the ship consists of Belytscho-Tsay shell elements, with the material model MAT_PIECEWISE_LINEAR_PLASTICITY. The material model will define an isotropic elasto-plastic material which can undergo plastic deformation.

The rear frame of the FE ship bow model is provided with the material model MAT_RIGID. This material model defines a rigid body and is a numerical technique to avoid any buckling in the ship frame during the impact. Since no deformations due to the impact are expected in the area, this material is used to provide the element with another density to give the ship bow model a mass that is equivalent to a fully intact ship. The material properties of the FE model are provided in Table 5.2.

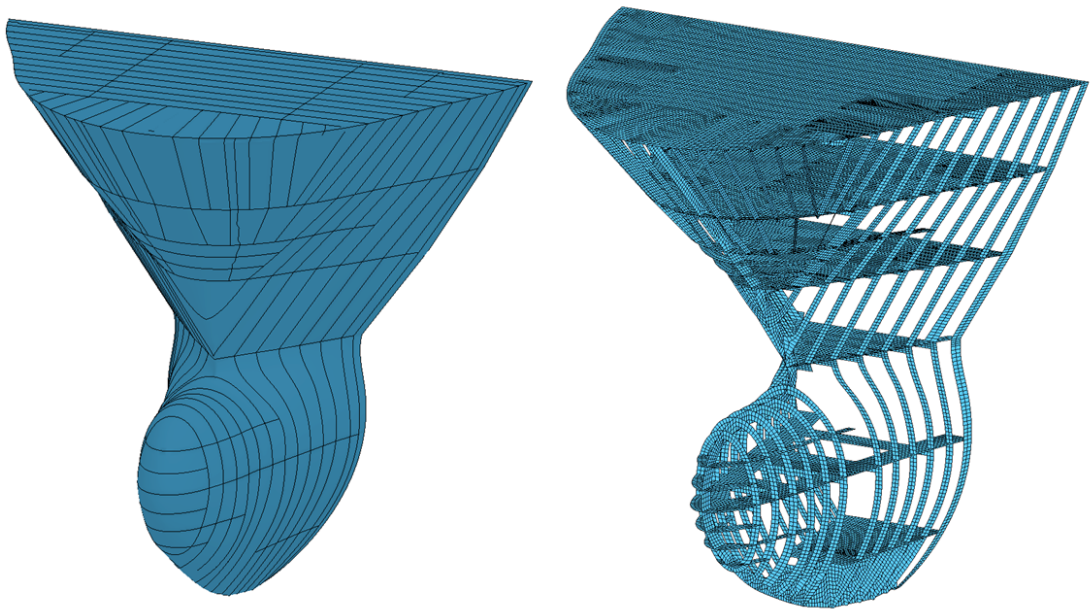

Figure 5.6: FE model of ship bow with structural mesh used in LS-DYNA.

Based on the historical ship traffic in the area and vessels colliding with Nordhordland Bridge earlier, this analysis will look into a cargo vessel with a displacement of 2000 tons as this is a realistic ship type for the area with high passage frequency. The displacement of the ship bow model is supposed to correlate to the displacement of an intact ship. The mass of the FE ship bow model is therefore set to 2000 tons. No added mass of the ship

bow is included in the FE model.

There is applied an initial velocity to the ship by using the keyword INITIAL_VELOCITY_GENERATION. This defines an initial nodal point translation velocities using the nodal set ID's [4]. The initial velocity is set to 5 m/s. As the velocity has a relatively small influence on impact compared with the displacement mass of the ship, only one incoming velocity is therefore analysed. 5 m/s corresponds to approximately 9,7 knots, which is a bit over the average cruising speed of a typical cargo vessel in the area of Salhusfjord. The FE model of the ship bow is located as close to the pontoon model as possible, to avoid unnecessary simulation time and to make the impact occur when the initial speed is applied to the ship bow model.

Table 5.2: Material properties for ship bow model in LS-DYNA.

Material	Material Model	Properties	
Steel	MAT_PIECEWISE_LINEAR_PLASTICITY	Density	7800 kg/m^2
		Poisson's ratio	0.3
		Yield stress	275 MPa
		Young's modulus	200 GPa
		Tangent modulus	730 MPa
	MAT_RIGID	Density	4.08e^6 kg/m^2
		Young's modulus	200 GPa

5.5 CFRP Model

After simulating the first scenario of the analysis, the simulation exposes that the pontoon model is subjected to large plastic deformation during the impact. A strengthening method is suggested by applying a CFRP layer of meshed shell element to the entire surface of the curved concrete wall where the ship impacts. The mesh created for the composite layer has an identical element size as the RC pontoon model, approximately 50x50 mm.

The material model MAT_ENHANCED_COMPOSITE_DAMAGE is used for the composite model, and all the material properties used in the material model in LS-DYNA are presented in Figure 5.3. The material properties of the CFRP sheet are based on the composite layer used by Sha in his research of the CFRP strengthening method of

reinforced concrete pontoons against ship collisions [29].

Two different CFRP sheets were modelled, having different thicknesses, fibre orientations and placements on the pontoon model. The first CFRP model was placed on the outer surface of the pontoon, with a thickness of 4 mm and only one orientation of the fibres. The other CFRP model was placed on the inner surface of the pontoon, with a thickness of 8 mm and two-orientated fibres.

Table 5.3: Material parameters for CFRP model in LS-DYNA.

Material	Material Model	Properties	
CFRP	MAT_ENHANCED_COMPOSITE_DAMAGE	Density	1795 kg/m^2
		Poisson's ratio$_{ba}$	0.0127
		Poisson's ratio$_{ca}$	0.0127
		Poisson's ratio$_{cb}$	0.4900
		Shear modulus	4.8 GPa
		Young's modulus$_{longitudinal}$	138 GPa
		Young's modulus$_{transverse}$	5.5 GPa
		Compressive strength$_{longitudinal}$	713 MPa
		Compressive strength$_{transverse}$	26.4 MPa
		Tensile strength$_{longitudinal}$	1.095 GPa
		Tensile strength$_{transverse}$	84.4 MPa
		Shear strength	84.4 MPa
		Max tensile strain in fibre	2.3%

5.6 Boundaries and Contact Formulation

AUTOMATIC_SINGLE_SURFACE is used to make sure there is self-contact between elements sharing surface. It is used in both the ship and pontoon model to maintain internal contact in the ship and the pontoon. No master is defined in the contact, only slave segments. The static coefficient of friction (FS) and dynamic coefficient of friction (FD) are set to 0.3. for each of the models. The friction coefficients are dependent on the relative velocity of the surfaces in contact [4].

To model the interaction between the ship bow and the pontoon bodies, the contact keyword AUTOMATIC_SURFACE_TO_SURFACE was utilized. As this is a two-way contact, a slave and a master is defined in the relation. Both FD and FS were set to 0.2 Remaining coefficients are set to default parameters for the contact keywords.

To ensure a contact relation between the CFRP layer and the surface of the concrete pontoon, the penalty-based contact keyword AUTOMATIC_SURFACE_TO_SURFACE

TIEBREAK is utilized, where the CFRP sheet is defined as the slave and the pontoon as the master. Both the coefficients of friction are set to 0.7 in the contact between the CFRP sheet and the concrete wall of the pontoon.

BOUNDARY_SPC_SET is used to apply desired boundary conditions on the chosen node sets of the pontoon. The nodes located at each of the four edges of the pontoon were assumed translation and rotational constraints about all local axis. This reflects the support from the other half of the pontoon, which not was modelled to save computational resources. For the reduced pontoon model all the edges were also assumed constrained in the same way. See figure 5.7. It was chosen not to constrain the ship bow model as a ship can move in all directions when floating in real situations.

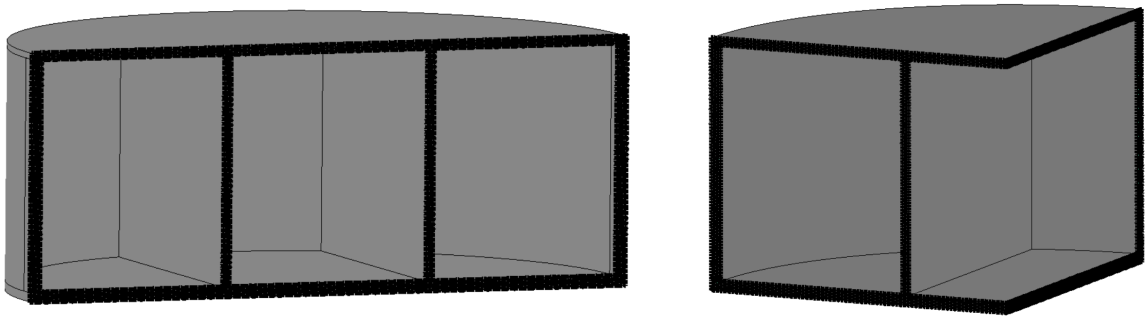

(a) **(b)**

Figure 5.7: Boundaries on the FE pontoon models

5.7 Validation of Material Model MAT_CSCM

The material model MAT_CSCM used for the concrete in the analysis is a well-known material model in LS-DYNA. The material model is chosen as it is widely used when simulating normal strength concrete under the impact of collisions. A verification of the behaviour of the material model was provided by Fan and Yuan in 2014 [48]. In their research, several concrete material models have been implemented in LS-DYNA and compared with experimental data from Fujikake et al. research in 2004 [49]. The research concludes that the behaviour of MAT_CSCM agrees well with the experimental results of the concrete behaviour compared to other material models of concrete in LS-DYNA. The reinforcement in the impact test is coupled to the concrete with the constraint LAGRANGE_IN_SOLID, as is used in this analysis as well. Further development of the

material model is followed by the user manual for LS-DYNA Concrete material model MAT_CSCM.

Material tests can be proposed for calibration purposes for more accurate validation of the material models in the FE model. This will be recommended as further work.

6 Results & Discussion

In the following chapter, the results of the numerical analysis conducted to investigate ship-bridge collision scenarios are presented. The findings in the analysis disclose the interplay between a ship and a bridge structure in a collision, highlighting important factors such as impact forces, impact energy, structural responses, and potential damage patterns characterized by plastic deformations. The results will be discussed continually as it is presented, giving a brief summary of the consequences at the end. Some suggestion to minimise the risk of ship collision is introduced, and possible modelling complexities and errors that may have affected the analysis is stated.

6.1 Impact Head-on the Centre of Pontoon

The results of the impact scenario where the ship is hitting head-on in the centre of the pontoon are presented in this section. The progression of the impact is visually illustrated in Figure 6.1.

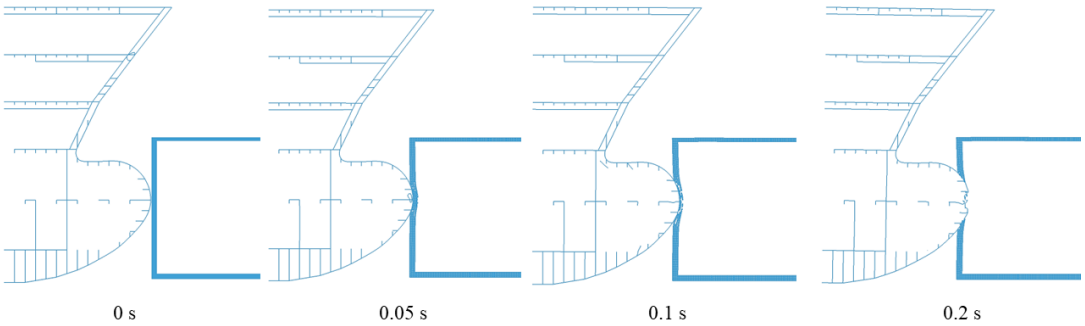

Figure 6.1: Development of head-on centre ship impact

At the area of contact from the ship bow, the pontoon wall experiences significant localized plastic deformation. However, the remaining sections of the pontoon do not exhibit significant damage. The pontoon is subjected to effective plastic strains through the impact as seen in the contour plot in Figure 6.2. From the figure, it can also be seen a typical occurrence of punching shear failure, where the capacity of the pontoon wall is lower than that of the ship bulb, resulting in a hole where the ship bow has impacted the pontoon wall.

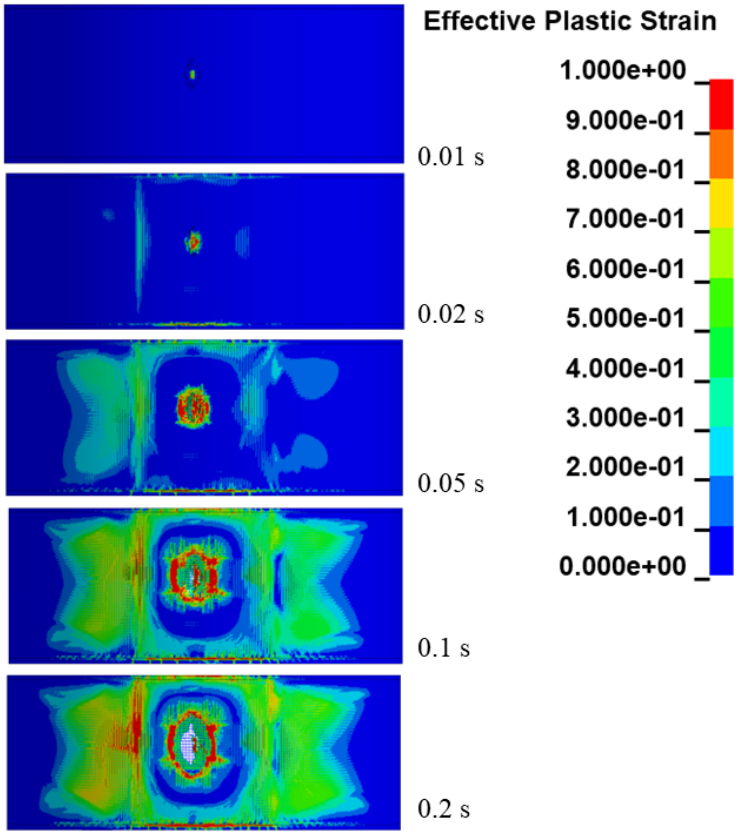

Figure 6.2: Effective Plastic Strain during head-on impact on the centre of the pontoon

The internal and kinetic energy obtained from the LS-DYNA analysis is shown in Figure 6.3. The primary objective of the analysis was to simulate a ship collision with an estimated impact energy of roughly 25 MJ, which corresponds to the assumed design capacity of the pontoons. As illustrated in Figure 6.3b and 6.4b, the total energy from the impact is precisely close to 25 MJ and the maximum impact force detected is approximately 14 MN. The gap between the internal and kinetic energy at 0.4 s, indicates that the ship will proceed to collide further into the pontoon wall. Some of the energy will be converted to sliding interface energy, spring and damper energy and system damping energy, but since these parameters represent a small part of the total energy, and is not the main target to address, there is concluded to neglect these in this presentation of the results.

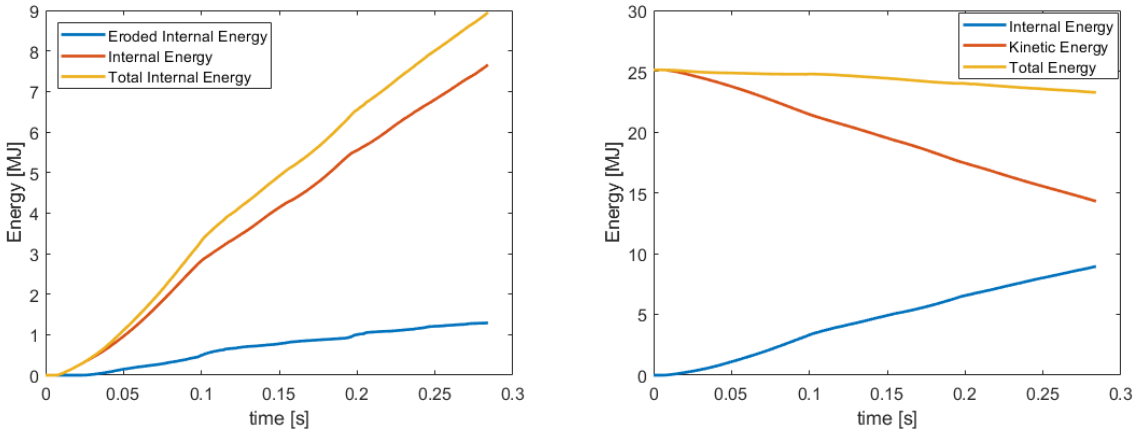

(a) Internal Energy **(b)** Total Energy

Figure 6.3: Impact Energy in head-on impact in the centre of pontoon

Based on the internal energy comparison between the two FE models shown in Figure 6.4a, it can be observed that the pontoon has less internal energy than the ship during the impact. This energy is absorbed by the pontoon, in the form of significant plastic deformations in the pontoon wall.

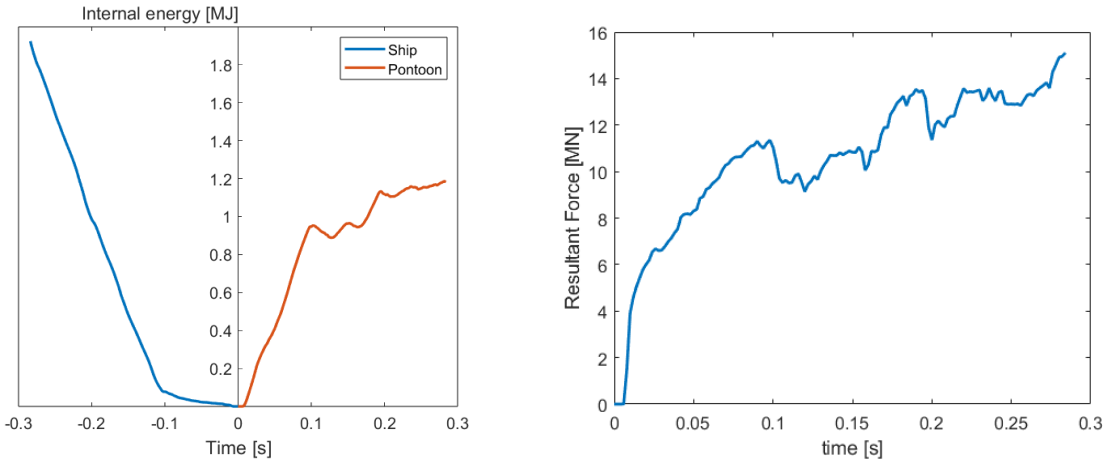

(a) Energy dissipation **(b)** Force of impact

Figure 6.4: Energy dissipation and impact force during head-on impact in the centre of the pontoon

The initial velocity of the ship at 5 m/s gradually decreases as it collides with the pontoon wall. There are variations in the measured velocity, depending on the location of the nodes on the ship bow model. Figure 6.5 illustrates that the frontal node experiences disturbances such as vibrations due to the impact.

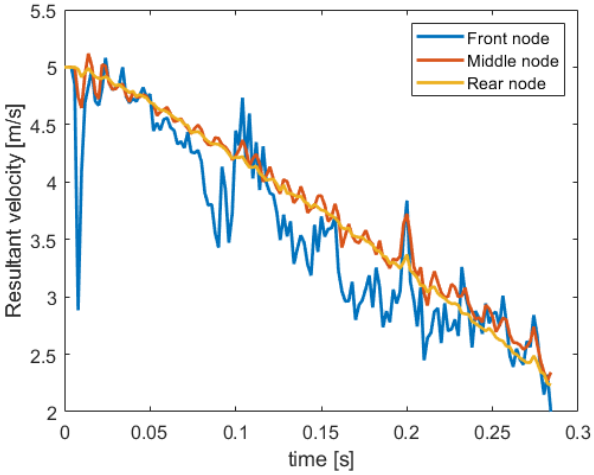

(a) Velocity in impact, 3 different nodes

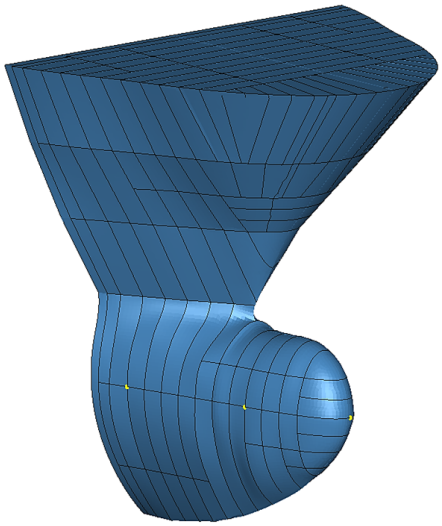

(b) Ship bow model with front, middle and rear node marked in yellow

Figure 6.5: Development of velocity of head-on towards centre impact

The simulation where stopped by time limitations after 20 hours of computation. During this computed time, only 3.5 MJ of the collision energy is absorbed through structural damage to the pontoon wall in the analysis. Consequently, the ship retains a substantial amount of kinetic energy and will proceed to collide further into the pontoon wall, resulting in continuous crushing.

Since this scenario resulted in the collapse of the pontoon wall, it was concluded that there is no need to conduct further simulations with larger ship displacements. The next planned simulation with a ship displacement of 3000 tons was therefore unnecessary.

6.2 Impact Head-on the Inner Wall of Pontoon

In this section, the results of the impact where the ship hits the pontoon off-centre, head-on towards the internal concrete walls of the cells inside the pontoon, are presented. The progression of the impact scenario is shown in Figure 6.6.

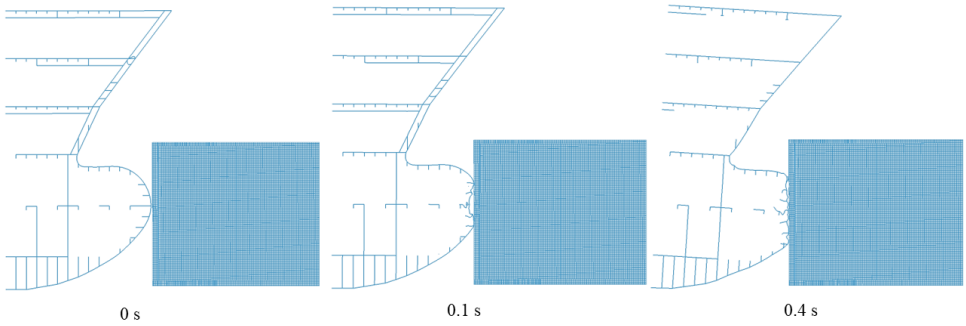

Figure 6.6: Development of impact head-on to the inner concrete wall of pontoon

Hitting the pontoon head-on off the centre produces a markedly different outcome compared to the head-on centre scenario. The ship bow experiences large plastic deformation in the impact as illustrated in Figure 6.7a, while there is almost no deformation on the concrete wall or at the internal structure of the pontoon. Even if the pontoon does not have severe deformations, it is subjected to strains, as shown in Figure 6.7b.

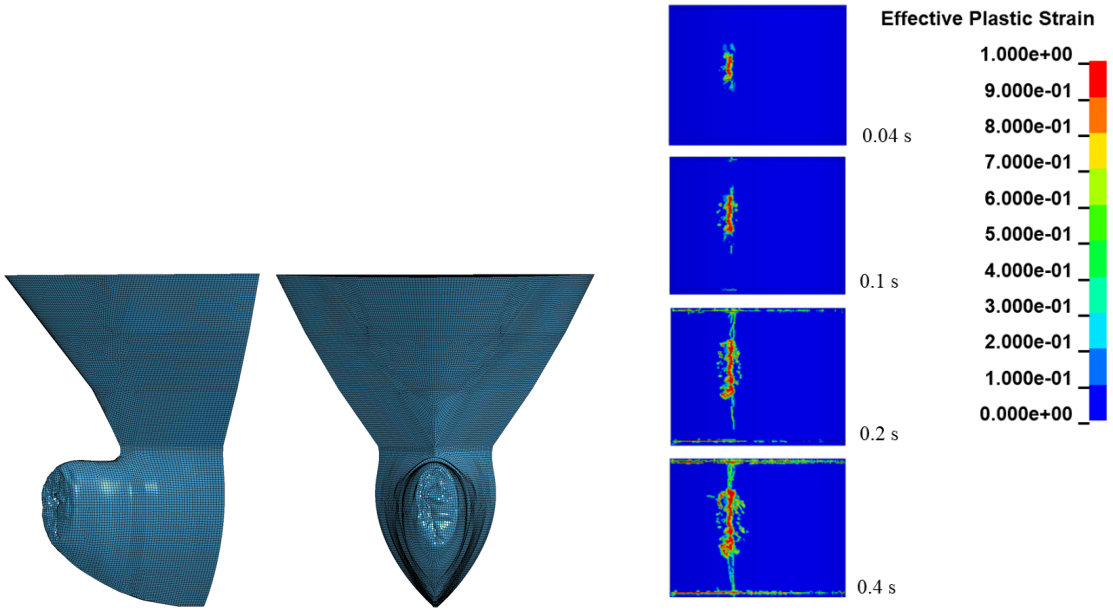

(a) Ship Damages after impact **(b)** Effective Plastic Strain after

Figure 6.7: Ship impact head-on to the inner concrete wall of the pontoon

The internal and kinetic energy values obtained from the LS-DYNA analysis are presented in Figure 6.8. The total energy of the impact is also 25 MJ in this impact scenario. Looking at the difference of the internal and kinetic energy 0.4 s into the impact, the difference in the energy balance indicates energy absorption in some form, but to a much lesser extent than for the head-on centre scenario. Less plastic deformation occurs in the pontoon, and this is also indicated by the eroded internal energy in Figure 6.8a.

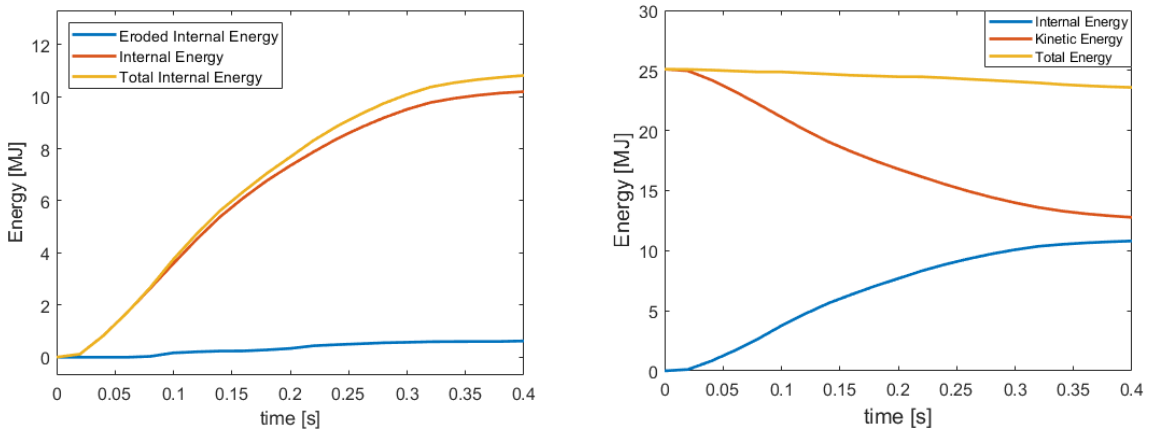

(a) Internal Energy **(b)** Total Energy

Figure 6.8: Impact Energy in the head-on impact towards the inner wall of pontoon

From the energy dissipation of this impact in Figure 6.9a, it can be observed that a lot of the energy is absorbed in the ship bow model compared to the pontoon model. The impact force illustrated in Figure 6.9b gradually drops to 0 MN after 0.6 s, as the ship bow absorbs the energy of the collision and undergoes further deformation.

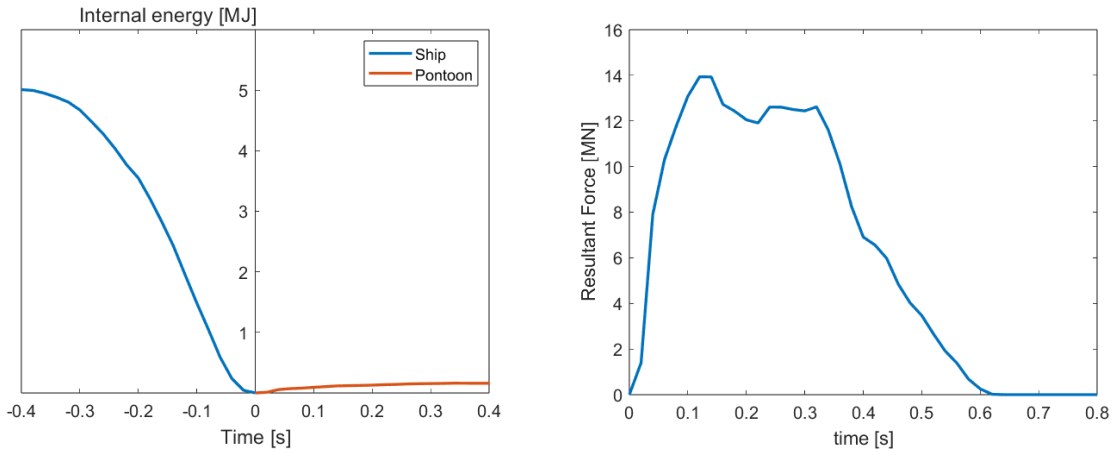

(a) Energy dissipation **(b)** Force of impact

Figure 6.9: Energy dissipation and impact force during head-on impact towards the inner wall of the pontoon

The velocity of the ship bow model drops quite fast when hitting the pontoon wall as seen in Figure 6.10. After 0.4 s of the impact, the ship bow model starts to tip over. This can also be seen in Figure 6.6. This gives an increase in the resultant velocity of the ship.

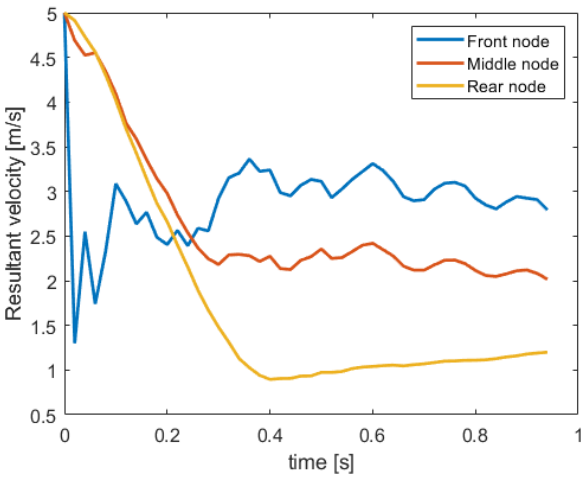

(a) Velocity in impact, 3 different nodes

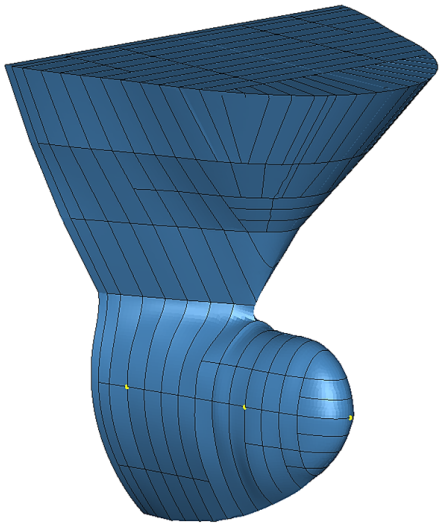

(b) Ship Bow Model with front, middle and rear node marked in yellow

Figure 6.10: Development of velocity in head-on impact towards inner wall

6.3 Glancing Blow

The results of the scenario of a glancing blow impact are described in this section. The evolution of the impact can be seen in Figure 6.11. As this scenario is not a head-on impact but a glancing blow, the pontoon will force the ship out to the side. This scenario is most like the one collision that actually occurred at Bergsøysund Bridge in March 2023.

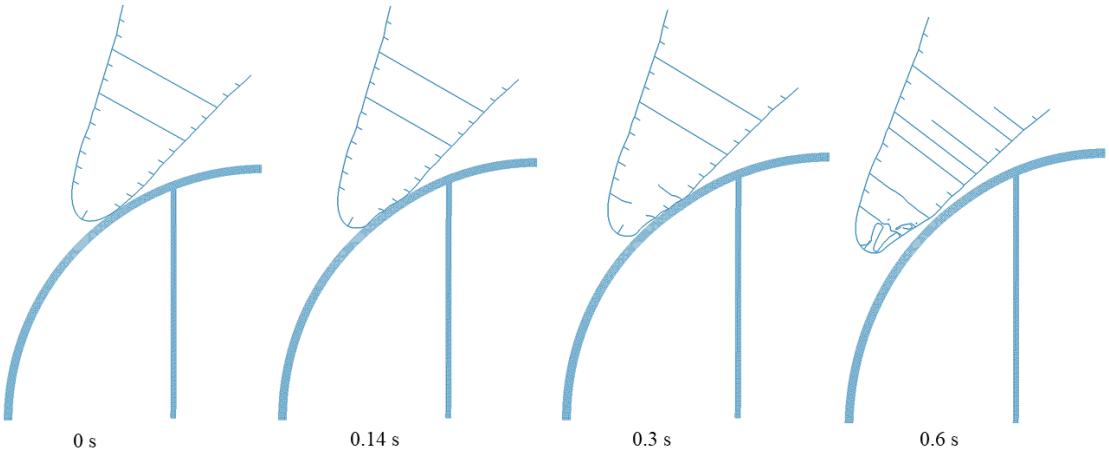

Figure 6.11: Top view of the development of glancing blow impact

The total internal and kinetic energy from the analysis of the impact is illustrated in Figure 6.12. Internal eroded energy indicates no damage of a significant degree, but there is still a large gap between the energy balance in Figure 6.12b.

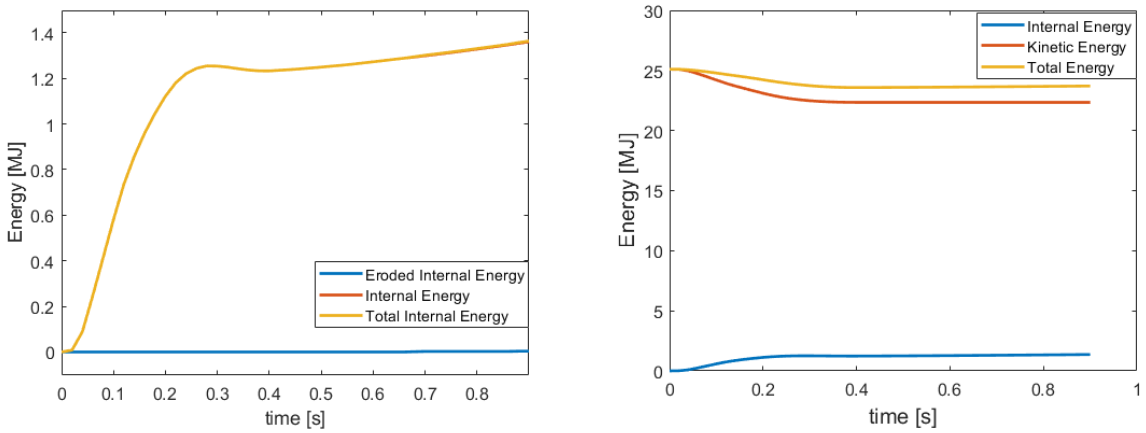

(a) Internal Energy **(b)** Total Energy

Figure 6.12: Impact Energy in the glancing blow impact of the pontoon

The maximum force of impact during the glancing blow is 6.64 MN as seen in Figure 6.13b. The impact force drops drastically after 0.2 s as the ship separates from the pontoon and is exposed to plastic deformations. Figure 6.13a illustrates the energy dissipation of the impact.

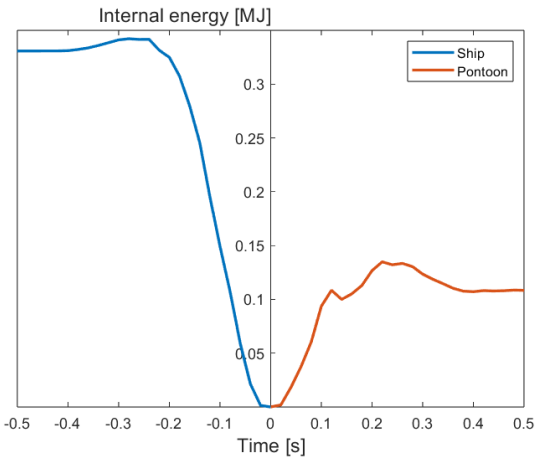

(a) Energy dissipation

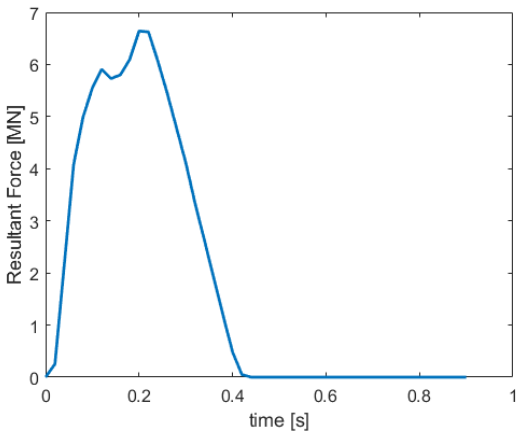

(b) Force of impact

Figure 6.13: Energy dissipation and impact force during the glancing blow impact of the pontoon

The velocity of the ship bow model is given in Figure 6.14. The increase of the resultant velocity of the front node occurs when the ship bow is being pushed slightly in the perpendicular direction to the incoming velocity as it hits the pontoon.

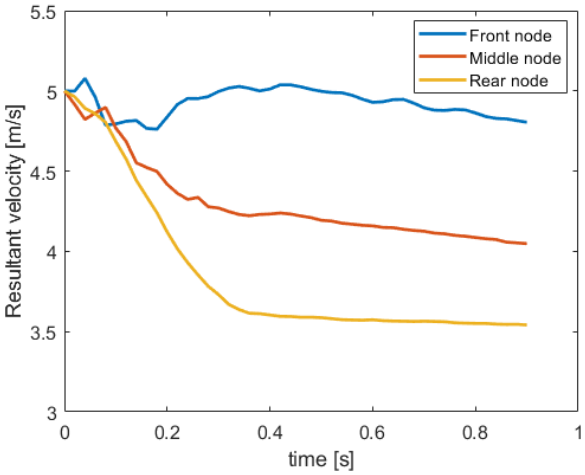

(a) Velocity in impact, 3 different nodes

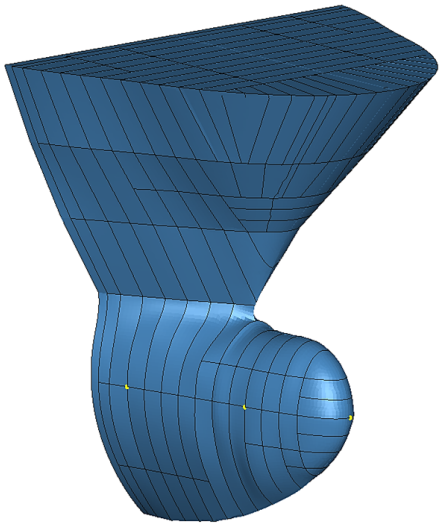

(b) Ship Bow model with front, middle and rear node marked in yellow

Figure 6.14: Development of velocity in glancing blow scenario

Most plastic deformation in the ship bow during impact as seen in Figure 6.15a, but small damages compared to the other scenarios. No significant deformation on the pontoon wall or internal structures in the glancing blow, but is subjected to effective plastic strain, as shown in Figure 6.15b.

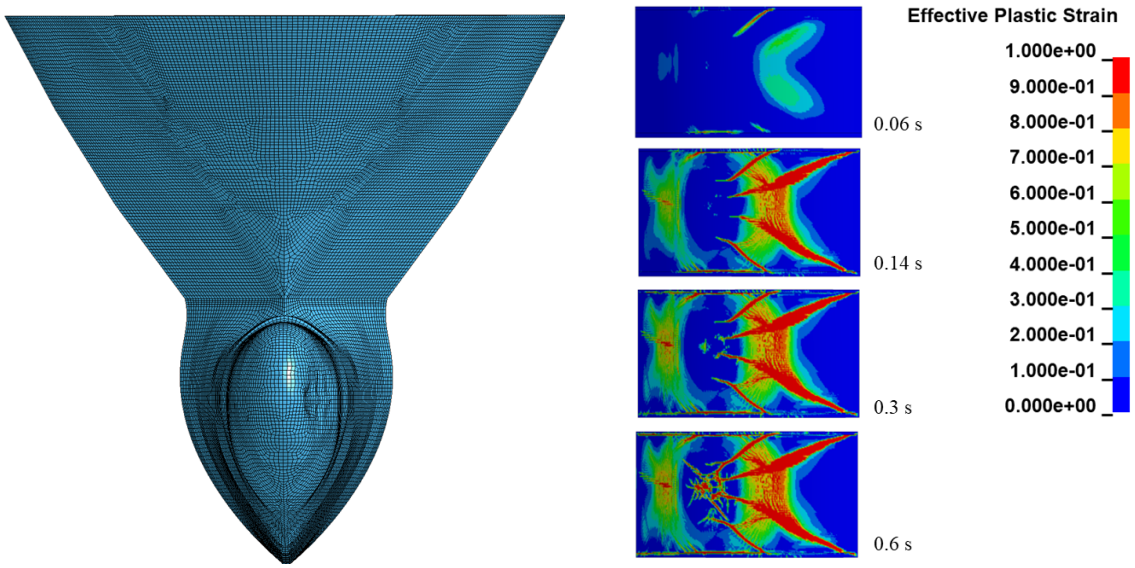

(a) Plastic deformation on striking side of ship bow model

(b) Effective plastic strain contours of the glancing blow

Figure 6.15: Ship impact of a glancing blow

6.4 CFRP Strengthening

In this section, the result of the strengthening method on the head-on impact in the centre of the pontoon is described.

6.4.1 CFRP 4 mm

The total impact energy of the CFRP sheet of 4 mm, placed on the outside of the pontoon wall is presented in Figure 6.16. The evolution of the impact energy from 0 to 0.1 s tends to develop very much like the head-on centre simulation without a sheet of CFRP. The velocity of the ship bow model gradually reduces, with disturbance as seen in Figure 6.17.

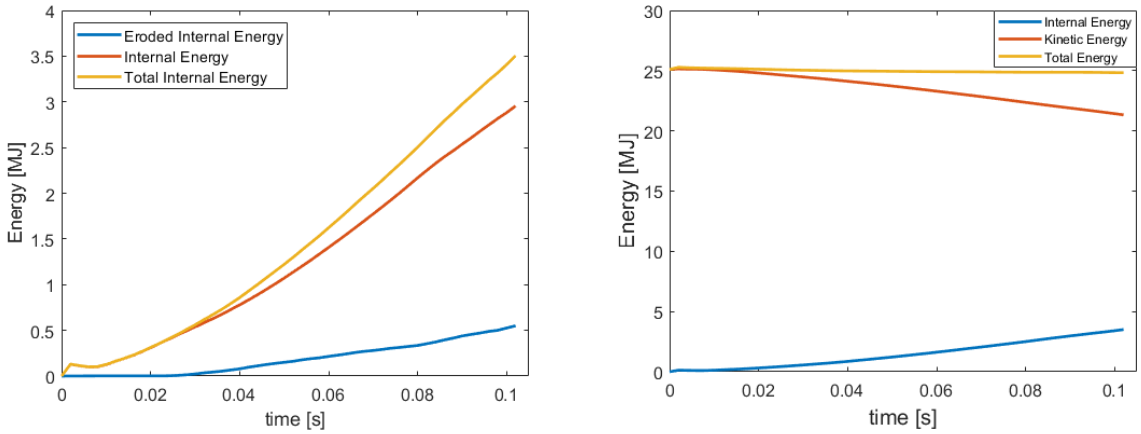

(a) Internal Energy **(b)** Total Energy

Figure 6.16: Impact energy in head-on centre impact with CFRP 4 mm

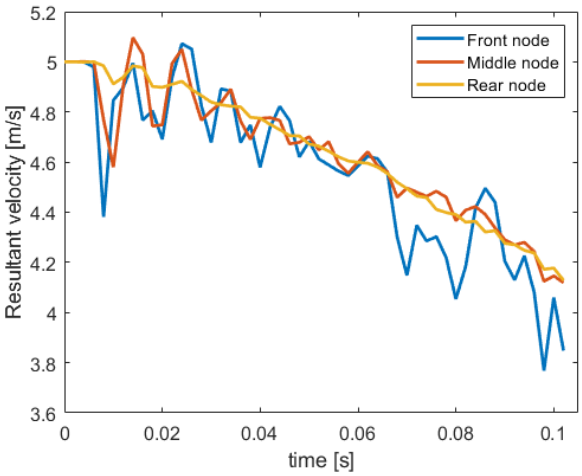

(a) Velocity in impact, 3 different nodes

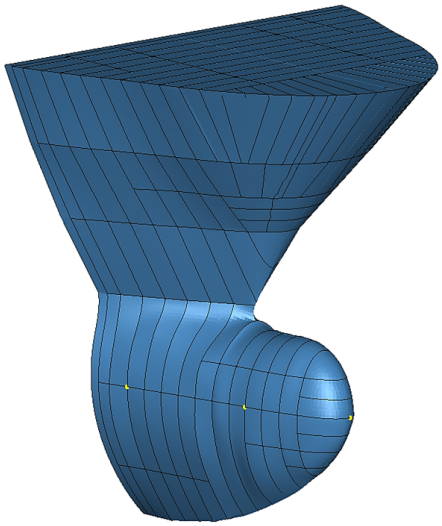

(b) Ship bow model with front, middle and rear node marked in yellow

Figure 6.17: Development of velocity of head-on impact with CFRP 4 mm

Even with the application of a strengthening layer of CFRP, the pontoon wall still experiences significant effective plastic strains, as seen in Figure 6.18. It forms an unexpected distribution of effective plastic strain all over the surface of the pontoon during the impact.

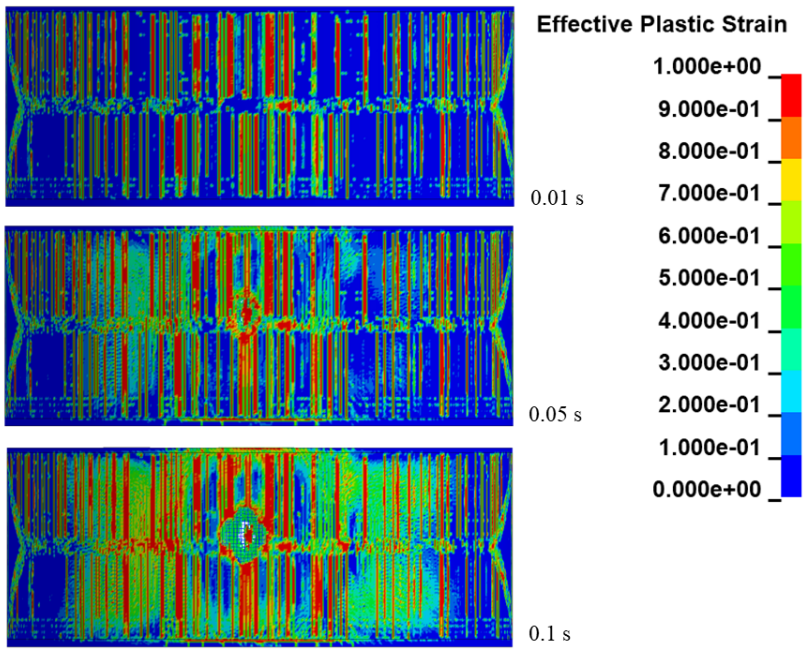

Figure 6.18: Effective plastic strain of head-on centre impact with CFRP 4 mm

The energy dissipation and impact force given in Figure 6.19, are nearly equal to the result from the simulation without the CFRP. A small increase in the internal energy of the pontoon is expected as the CFRP sheet is attached to the model.

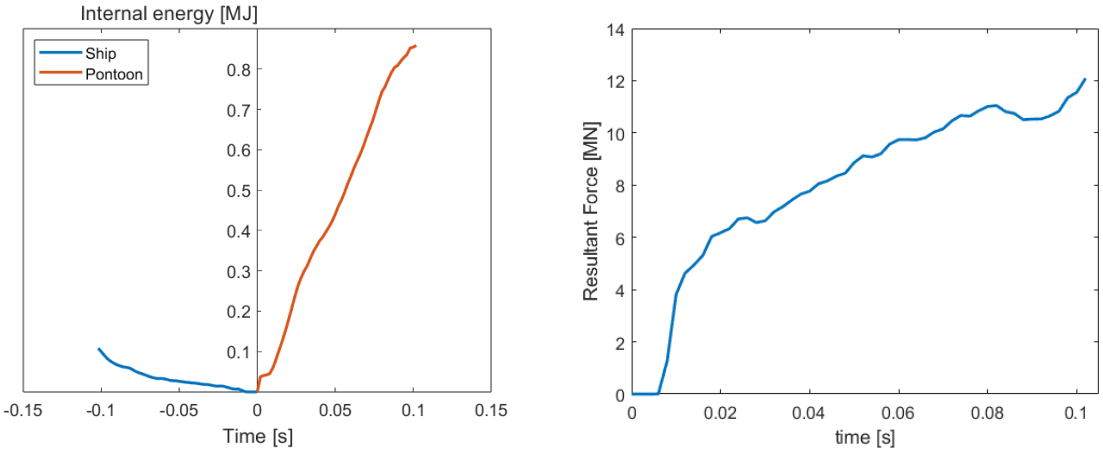

(a) Energy dissipation **(b)** Resultant force

Figure 6.19: Energy dissipation and impact force during head-on impact in the centre with CFRP 4 mm

6.4.2 CFRP 8 mm

The total impact energy of the CFRP sheet of 8 mm, placed on the inside of the pontoon wall is given in Figure 6.20. Due to challenges to the simulation, only a very short period of the impact is simulated in the analysis. The evolution of the impact energy from 0 to 0.06 s tends to look similar to the other head-on centre impacts in the initial stage of the collision. Even with the application of a strengthening layer of CFRP, the pontoon wall still experiences effective plastic strains, as shown in Figure 6.21.

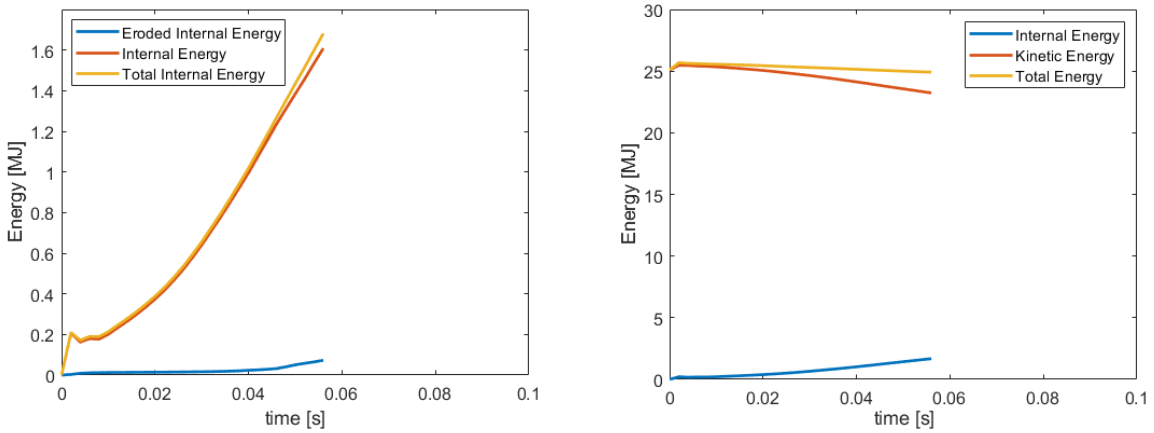

(a) Internal Energy **(b)** Total Energy

Figure 6.20: Impact energy in the head-on impact in the centre with CFRP 8 mm

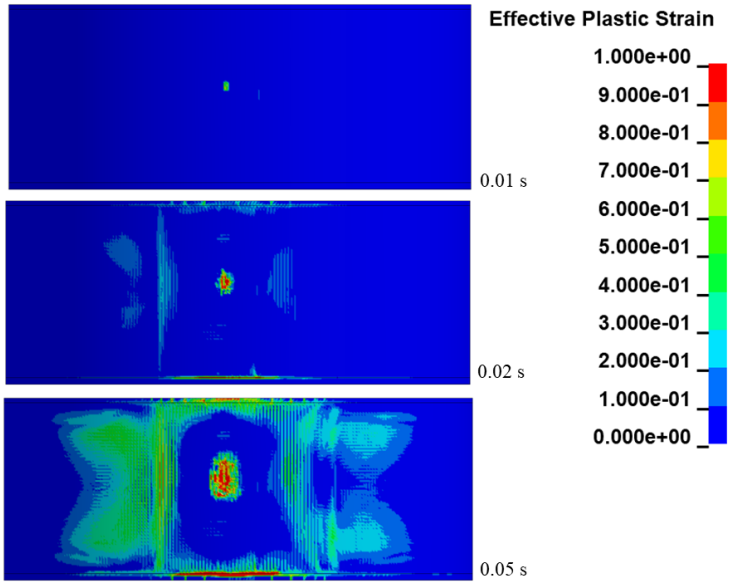

Figure 6.21: Effective plastic strain contours from head-on centre impact with CFRP 8 mm

The velocity of the ship bow model in Figure 6.22 shows how the frontal node of the ship bow gets the velocity decreased drastically when getting in contact with the pontoon surface with a CFRP sheet on the backside.

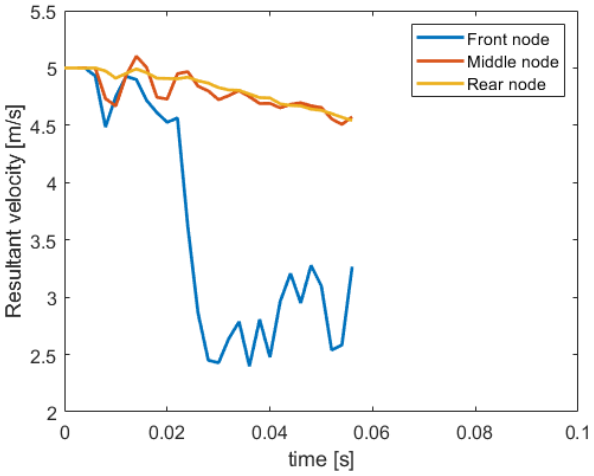

(a) Velocity in impact, 3 different nodes

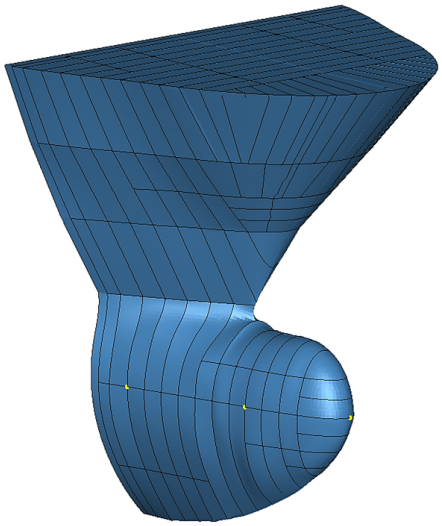

(b) Ship bow model with front, middle and rear node marked in yellow

Figure 6.22: Development of velocity of head-on towards centre impact with CFRP 8 mm

The energy dissipation and impact force are given in Figure 6.23. In the figure, there can be seen a slight increase in the internal energy for the pontoon here well, as the CFRP sheet is added to the model. The slope of the curve showing the energy dissipation for the ship has a large increase compared to the head-on impact without CFRP. The ship reaches the same energy dissipation in 0.06 s as for 0.12 s in the scenario without CFRP. There is also an increase in the impact force in this scenario, as it reaches roughly 12 MN already at 0.05 s.

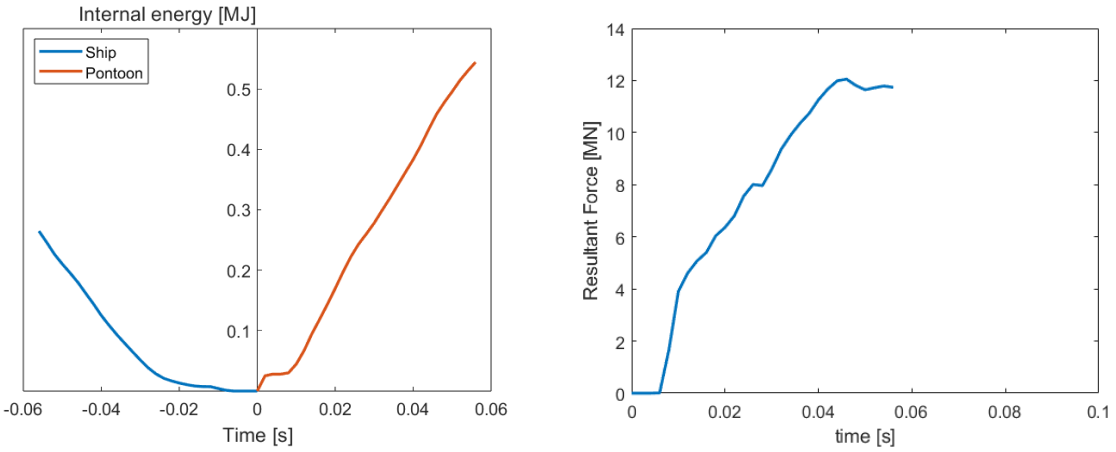

(a) Head-on centre CFRP 8 mm **(b)** Resultant force

Figure 6.23: Energy dissipation and impact force during head-on centre impact with CFRP 8 mm

During this simulation, it is observed that only a fraction of the collision energy is absorbed by the structural damage to the pontoon wall. As a result, the ship retains a significant amount of kinetic energy and continues to collide with the pontoon wall, leading to ongoing crushing and deformation as in the head-on centre impact.

6.4.3 Effect of Strengthening

There is a noticeable disparity in the effective plastic strain between the two different CFRP layers. Figure 6.24 illustrates the development of the effective plastic strain from 0.01 to 0.05 seconds in the impacts with different CFRP sheets. It should be noted that due to the limited simulation time for the 8 mm CFRP layer, only the first 0.06 seconds of the impact is compared.

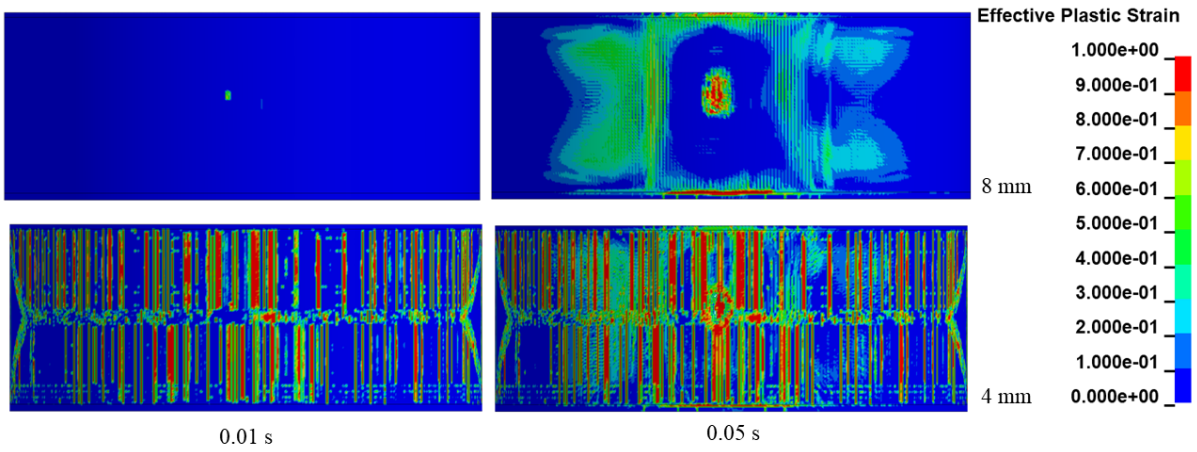

Figure 6.24: Comparison of the two different CFRP layers

When comparing the simulation of the CFRP-strengthened model with an 8 mm thickness (Fig. 6.25b)to the simulation of the model with a regular RC wall (Fig. 6.25a), an effect of the CFRP can be observed in Figure 6.25. The comparison reveals a delay in the plastic deformation and less concentration of effective plastic strain in the model with an 8 mm CFRP sheet applied to the rear surface of the pontoon wall.

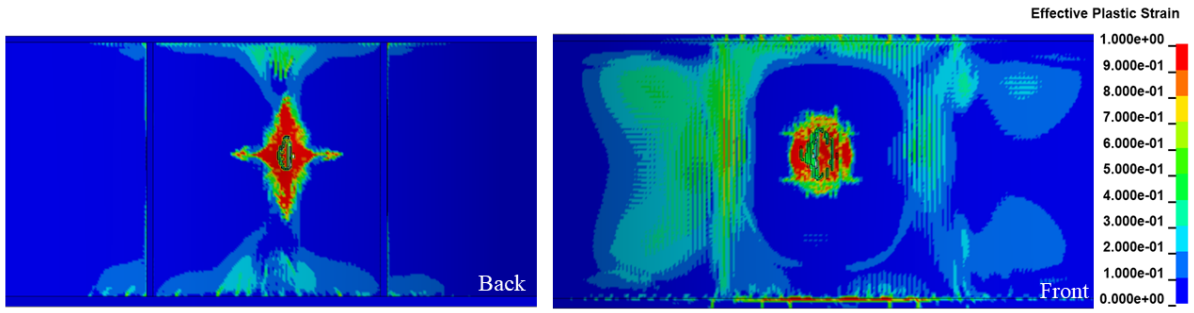

(a) RC pontoon

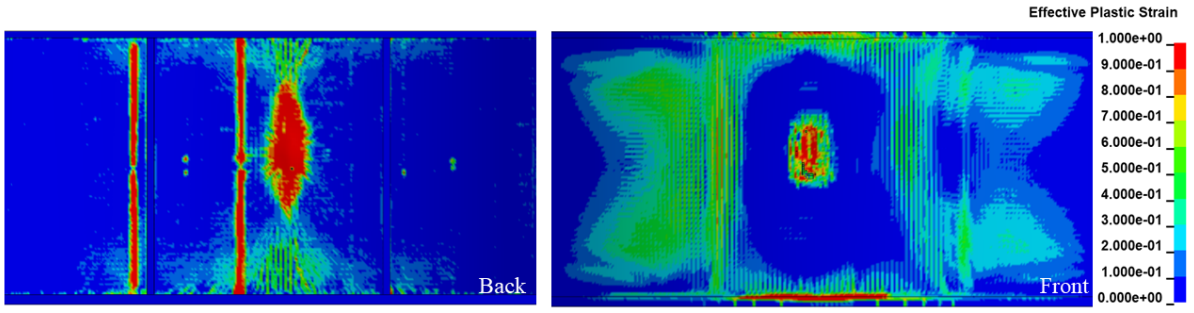

(b) RC concrete pontoon with CFRP sheet 8 mm

Figure 6.25: Effective plastic strain contours of RC pontoon without (a) and with (b) CFRP of 8 mm at 0.05 s

The results of the CFRP sheet of 8 mm indicate a positive trend, suggesting that the approach employed may have a beneficial effect. However, due to the limitations of computational time, it remains uncertain whether this approach will merely delay the occurrence of punching shear failure or effectively prevent the damages from occurring altogether.

In the CFRP layer with 4 mm thickness, placed at the front surface of the pontoon there is less effect. As the effective plastic strain development is clearly affected by the contact between the CFRP sheet and the pontoon wall, it is difficult to do a straight comparison in the area of impact in the front. On the back side of the impact, it is a very small effect of the CFRP sheet of 4 mm evaluating the effective plastic strain contours in Figure 6.26.

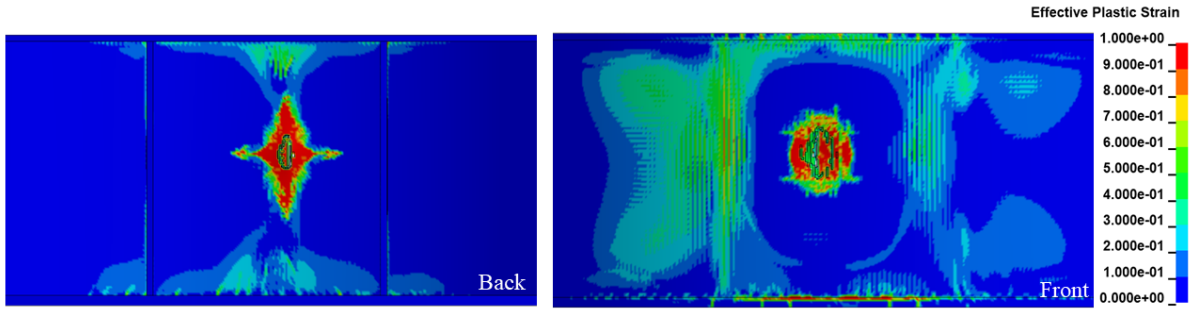

(a) RC pontoon

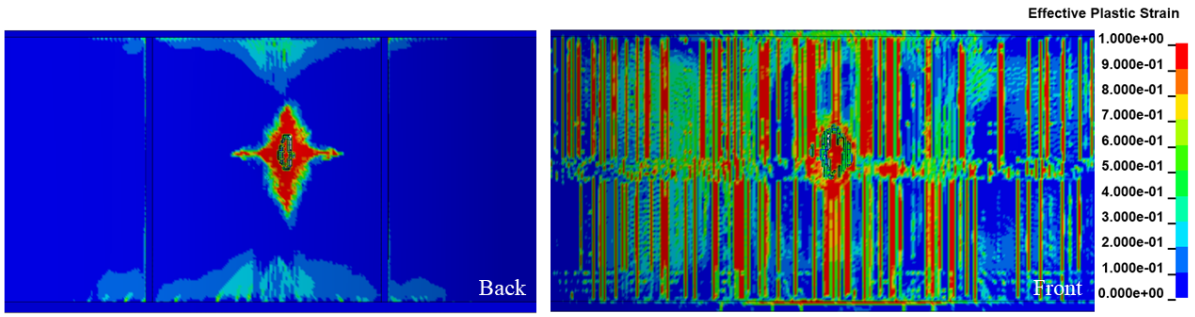

(b) RC concrete pontoon with CFRP sheet

Figure 6.26: Effective plastic strain contours of RC pontoon without (a) and with (b) CFRP of 4 mm at 0.05 s

Even for the short simulation, it can be concluded from the results that the placement and thickness of the CFRP are crucial. No effects on the outside, as the fibre placement and orientation affect the strength and stiffness of the CFRP.

6.5 Force-displacement Curves

Considering the local response of the RC pontoon wall, Figure 6.27 presents the force-displacement plots for the different scenarios simulated in the analysis. It can be observed from the curves, that all the head-on centre scenarios obtain the same force-displacement relation the first 0.09 m of displacement, then they start develop differently. As there is very little effect of the CFRP sheet of 4 mm, the force-displacement curve follows the head-on centre scenario similarly for the simulated period.

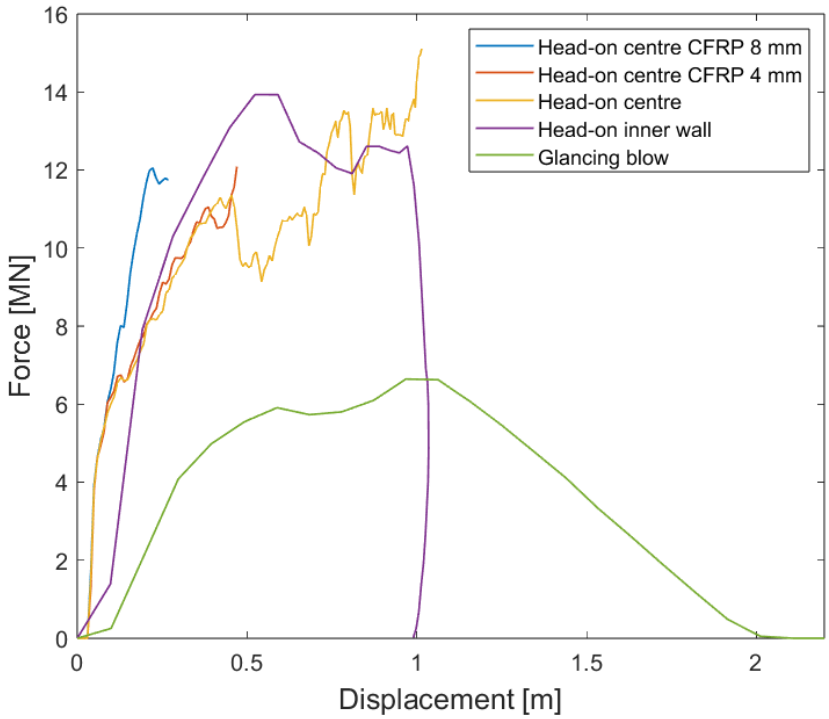

Figure 6.27: Force-displacement relation of all impact scenarios analysed

The force gradually decreases as the ship's structure starts to absorb the energy of the collision and undergoes further deformation. Eventually, the force reaches a point where the ship's structure can no longer resist the displacement, and the force decreases rapidly as the ships separate. This can be observed by the glancing blow and the impact head-on the inner wall of the pontoon. These were the only simulations that actually were able to run the entire analysis within the given CPU hours in the computation. For the head-on centre impact scenarios, there is difficult to see anything else than the tendency, because of the short run of analysis.

6.6 Energy Dissipation

Figure 6.28 presents the energy relation over time between the ship bow and the pontoon. There is a substantial difference in the internal energy of the ship bow model for the different scenarios. The energy dissipation plot agrees with the plastic damages in the ship observed from the result, as well as the damages to the pontoon as the glancing blow and head-on towards the inner wall impacts give insignificant damages compared to the head-on impact to the centre of the pontoon. The large difference in the internal energy of the pontoon can be explained by the reduction of elements in the FE model for the two analyses of the glancing blow and the head-on inner wall impact, as only a quarter of the initial model was used to save computational time.

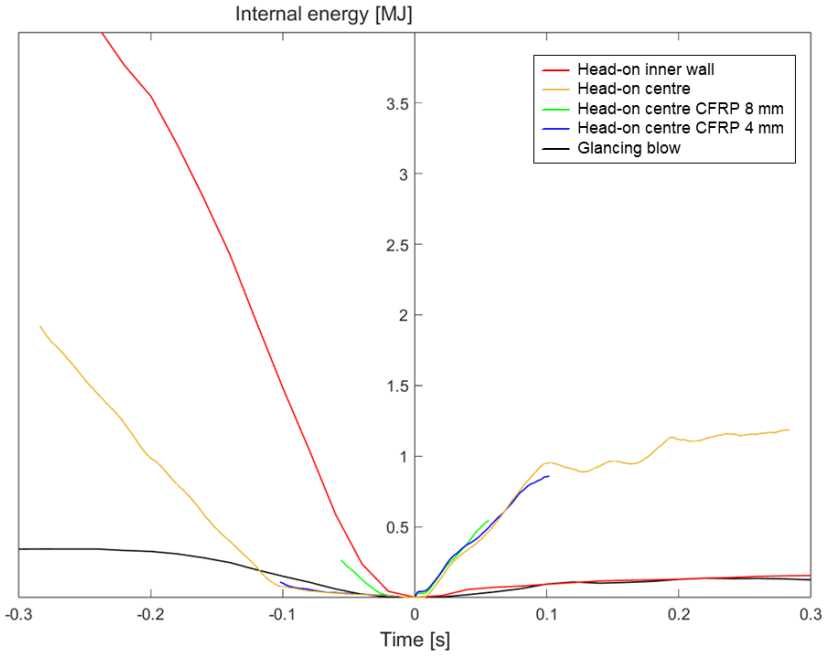

Figure 6.28: Energy dissipation for all impact scenarios analysed

6.7 Hourglass Verification

As mentioned in the review of the finite element method in Chapter 3.1, the hourglass energy should be kept under 10% of the internal energy to be valid [34]. To validate the FE models in this research, the total hourglass energy is compared to the total internal energy in each scenario simulated. In Figure 6.29 all five different impact scenarios are presented. As seen from the figure, the hourglass energy is less than 10% of the total internal energy for all scenarios except the two simulations with a strengthening sheet of CFRP added (Fig. 6.29c & 6.29d).

Contact and boundary conditions have a large impact on the accuracy. Hourglass energy can decrease when refining the mesh. A problem with the model with CFRP sheets may have been that the mesh being too coarse.

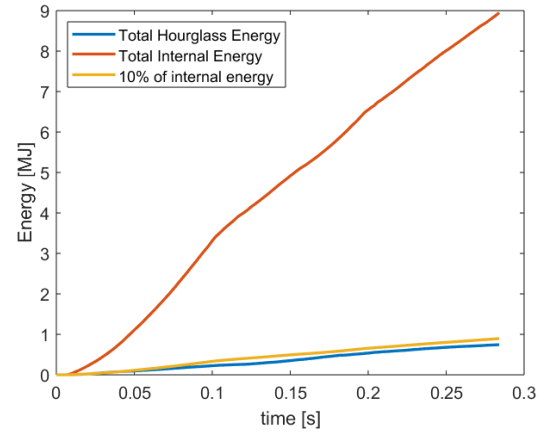

(a) Head-on centre impact

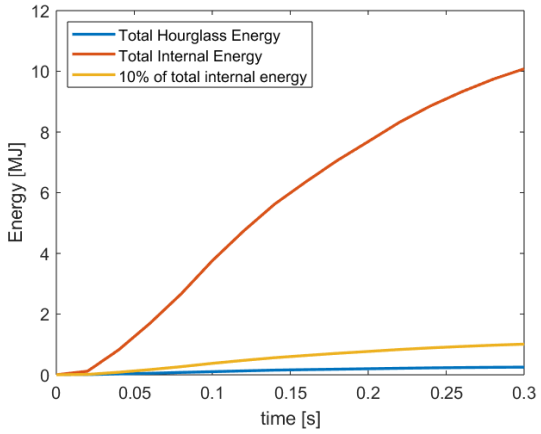

(b) Head-on towards inner wall impact

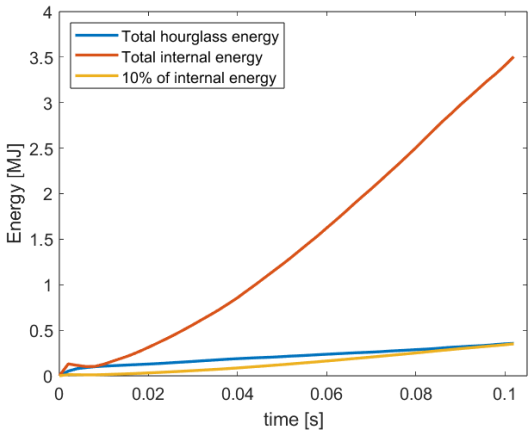

(c) Head-on impact at the centre of pontoon with strengthening CFRP 4 mm

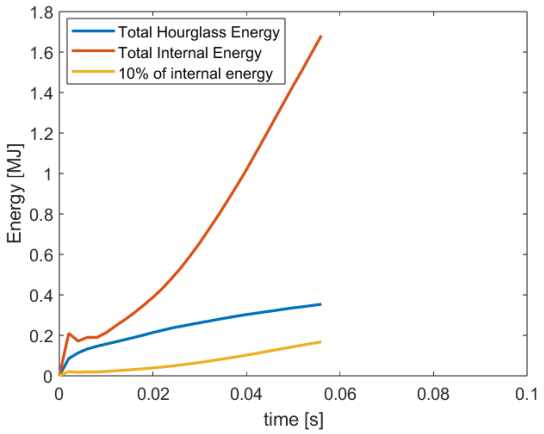

(d) Head-on impact at the centre of pontoon with strengthening CFRP 8 mm

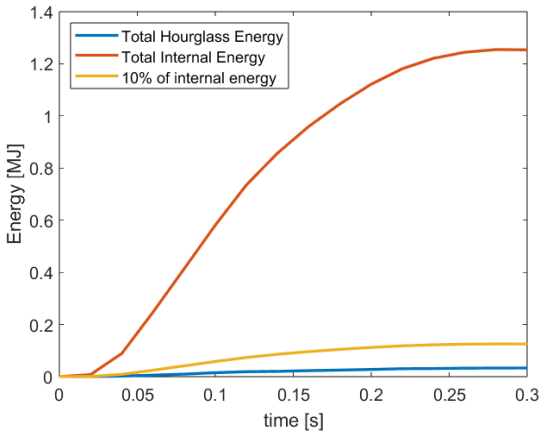

(e) Glancing blow

Figure 6.29: Hourglass verification of all impact scenarios

6.8 Consequences of the Ship Impact

The head-on impact in the centre of the pontoon gives a total impact energy of 25 MJ from the numerical analysis. Even if the pontoons are designed to withstand an impact energy of 25 MJ, it is subjected to severe damage in the analysis. The 310 mm thick RC wall in the pontoon is unable to safely resist the impact from the ship collision of this proportions. From the simulation, it is clear that the plastic deformation only appears mostly locally in the impact region of the pontoon. The local deformation is on the other hand so a severe degree that the affected cell will be flooded with seawater.

The design of the cells in the pontoon ensures that even in the event of significant damage where two neighbouring cells out of the total nine cells are filled with water, there will still be no threat to the rest of the bridge. Taking this into consideration, the analysis of approximately 0.3 seconds of the impact performed in this thesis poses no threat to the integrity of the remaining structure on the bridge. Since the further development of this impact is unknown, it is essential to gather data for the entire sequence of events to conduct a comprehensive global analysis of the bridge.

Since the two collisions at the Nordhordland Bridge involved the deep water foundation and the bridge girder, the collision at Bergsøysund Bridge provides the most suitable basis for comparison with the glancing blow scenario analyzed. Notably, neither the real-life incident nor the analysis resulted in severe damage to the pontoon. This emphasizes the significance of the incoming angle of the ship in ship-bridge collisions.

The impact head-on towards the inner wall of the pontoon implifies a hard impact, which is desired for a ship-bridge collision [10]. From the analysis, a large amount of the impact energy dissipated through deformation in the ship bow and internal hull structure as seen in the figures presented in Chapter 6.2. The outer surface and internal wall of the pontoon remain undamaged following the incident. This scenario can potentially get critical as two neighbouring cells can be flooded in case of large plastic deformations on the surface and internal wall of the pontoon.

The analysis indicates that the occurrence of less damage on the pontoons is evident when the incoming ship is capable of manoeuvring away from a head-on collision. The analysis also reveals that the divergence between the requirements and the actual performance of

the bridge is of a significant matter. As it is not mandatory to update risk analyses for existing bridges in Norway [1], this study highlights that existing bridges do not receive the necessary attention to preserve the safety in a developing society.

6.9 Suggestions for dealing with high-risk impacts

In this section, suggestions for dealing with the high-risk impact at the pontoons of Nordhordland Bridge will be given. Several risk-minimizing measures from existing research were proposed in Chapter 3.2.7.

It has been stated throughout the analysis that the largest risk for ship collision is closest to the navigational channel of the bridge. To reduce the risk of ship collisions, one of the actions suggested is an improvement of the navigational channel. This measure will not be directly related to reducing the risk of collision towards the pontoons at Nordhordland Bridge, as the pontoons are placed a distance from the navigational channel, and the fixed deep water foundation will be more exposed to these collisions. This will neither be a cost-effective action to reduce the probability of ship collisions at Nordhordland Bridge as it demands large reconstructions of the structure.

The pontoons are the weakest link of the structural bridge system in a floating bridge. For new floating bridges with concrete pontoons, a sufficient thickness of the pontoon wall must be considered. As it is difficult and not cost-effective to increase the thickness of the pontoons on existing structures, it must most likely be replaced to increase the capacity of the bridge [45]. Use of steel in the pontoons instead of concrete, which is planned for Bjørnafjorden Bridge, can also be beneficial [45].

As replacement of pontoons can be difficult and often not profitable, strengthening existing RC pontoons may therefore be a better choice for increasing the capacity of the bridge. As investigated in this paper, a protective layer of CFRP can increase the capacity of the concrete. A CFRP sheet with a thickness of 8 mm assigned on the inside of the concrete wall surface shows an effect on the capacity in the analysis. Based on the limited information provided, it is difficult to make a definitive statement about whether the simulation with CFRP only delays or reduces damages beyond the first 0.05 seconds of the impact. However, the information obtained from the analysis suggests a positive trend in improving the ship's capacity to withstand damage. To draw a meaningful conclusion

about the bridge's global state, it would be necessary to extend the simulation time beyond 0.05 seconds and assess the ship's response to the impact over a longer duration.

It is recommended to consider implementing VTS systems or other collision alert systems for existing floating bridges in Norway as a measure to mitigate the risk of ship collisions. As mentioned earlier in the paper, this approach appears to significantly reduce the probability of ship-bridge collisions and is cost-effective compared to the other alternative measures.

6.10 Modelling Complexities & Errors

There are a lot of parameters and possible errors that can have affected the analysis in this paper. Modelling complexities and errors can have occurred as a consequence of the researcher being a new user of LS-DYNA. It took a lot more time to get familiar with the software and understand the concept and complexities of the keywords used in the FE model than expected. Also, long and expensive computation time to simulate the model of the ship impact set limitations for attempts. The average time for computations of the scenarios with the entire pontoon model was 20 hours for 0.1 s of simulations. The model was improved by iterations, and shorter simulations were tested to check improvements, but not enough to see the whole collision mechanism in all cases as planned. As a result of this, the model was simplified and reduced in elements. Considering that the ship will hit somewhere in the middle of the pontoon, it was concluded that these details had an insignificant impact on the result from the collision simulation due to the position of the hit.

The simplification of most matter is the prestressing of the concrete pontoon. As pointed out in the limitations of this research, the pontoon is modelled with only reinforcement and no prestressing. This choice was made considering the complexity of the modelling compared to the experience of the researcher and the limited time. As the results are affected by this, the analysis in this thesis is more conservative and illustrates a kind of worst-case scenario as there would be an advantage to have prestressing and the pontoon model would most likely have been subjected to less damage.

The ship bow model tilted after hitting the pontoon model in some of the simulations, leading to data that is not suitable for analysis. To prevent this, the material model

MAT_RIGID could be utilized to constrain the rear frame of the ship, allowing movement solely in the x-direction. The initial velocity of the ship was 5 m/s. However, due to the absence of constraints, the resultant velocity slightly increased during these impacts as the ship acquired velocity along the y- and z-axis as well.

Another issue to consider regarding the boundary conditions is in the simulations with only a quarter used of the pontoon model. This applies to the glancing blow and the impact head-on toward an internal concrete wall. The impact in these scenarios occurs quite near the constrained edges of the pontoons, compared to when the half pontoon model is used in the head-on impact in the centre. The translation and rotational constraints about all local axis of the pontoon may have affected the results into a less conservative measure.

In retrospect, the mesh of the pontoon model should be divided into different sizes to reduce computational time and cost. Discretization errors in the meshing can have affected the result. In other words, by not implementing enough elements in the area of impact. The FE model should have been verified with a mesh sensitivity study, but due to time limitations, this is not conducted. A mesh sensitivity study is used to verify if the result from the analysis is sufficiently accurate and that it represents all relevant failure modes. Generally, a mesh refinement study is done by checking that the results are sensible stable by redoing the analysis with half element size [33]. This will be proposed as recommended further work.

7 Conclusion

This paper has investigated a ship-bridge collision at Nordhordland Bridge. The impact response of a reinforced concrete pontoon and a CFRP-strengthened reinforced concrete pontoon has been studied. Through a comprehensive analysis of existing literature and research and a case study in the form of numerical analysis, several key findings have emerged. The findings of the study can be summarized as the following:

The analysis indicates that the probability of ship collisions at Nordhordland Bridge is of such a degree that consideration must be taken. Therefore, evaluating the capacity of the pontoons is an essential step in conducting a risk assessment for Nordhordland Bridge.

Despite several modelling complexities and errors, the analysis reveals that a head-on impact in the centre of the pontoon wall, involving a ship with a displacement of 2000 tons and an incoming speed of 5 m/s, leads to significant large plastic deformations. The pontoon experiences localized punching shear failure in the area of impact where the ship's bow hits. The findings indicate that the existing pontoon design is insufficient to withstand the head-on impact from a vessel with an impact energy of approximately 25 MJ.

To enhance the capacity of punching shear in the pontoon during the initial stages of the impact, a strengthening method utilizing a layer of Carbon Fiber Reinforced Polymer on the pontoon's surface is employed. The results show a tendency of a positive effect. However, due to the limited computational time, it is uncertain whether this approach will merely delay the occurrence of punching shear failure or prevent damages altogether in an extended time perspective.

Through the simulation of various scenarios, it is evident that the plastic deformation of the pontoon is significantly reduced depending on the location of impact from the ship bow. In the case of a head-on impact off centre, where an internal concrete wall is present inside the pontoon, the majority of the energy is absorbed by the ship in the form of large plastic deformations. This results in only minor surface damage on the pontoon.

Furthermore, when simulating a glancing blow, where the ship only strikes the side of the pontoon, both the ship and the pontoon experience even less damage. In this scenario, the

ship absorbs most of the energy, while the pontoon only sustains minor surface damage.

In the event of a head-on impact on the bridge, it is essential to consider the implementation of strengthening methods for the pontoons or other measures aimed at minimizing the risk associated with such ship impacts at Nordhordland Bridge.

This research highlights the importance of risk assessment of existing structures, as the design codes and demands constantly develop. By addressing the weaknesses of existing floating bridges, it can contribute to enhancing the safety and reliability of future floating bridge design, ensuring long-term viability.

During the research period, utilizing LS-DYNA software has provided the researcher with a deeper understanding of the principles and techniques underlying finite element analysis (FEA). There have been challenges related to model setup, result interpretation, and troubleshooting. Overcoming these challenges will sharpen the ability to analyze complex problems and think critically when employing FEA for complicated scenarios within structural engineering in the future.

7.1 Recommended further work

The results from the analysis conducted in this thesis reveal some weaknesses in the pontoon design of Nordhordland Bridge. As this affects the rest of the bridge structure, further work should focus on model improvements to make the analysis more accurate and a global analysis of the bridge:

1. Further development of a more accurate analysis with an improved FE model. A pontoon model containing more design details and prestressing to improve the capacity of the pontoon walls. Hydrodynamics and other environmental loads affecting the pontoon during the impact are to be included in the dynamic FEM simulation. More computational resources to expand the simulation time.

2. Mesh sensitivity study of the FE-model used in the numerical simulations to validate the accuracy of the model.

3. Material tests for calibration purposes of the material models in the FE model.

4. Global analysis to investigate the response and capacity of the bridge with all

elements when subjected to a ship collision towards the pontoons.

5. Investigate new materials and construction techniques of the pontoons to increase their capacity against ship collisions.

References

[1] M. E. Egeland, Y. Sha, I. Moen, and R. Flage, "Ship allision risk analysis for the 28-year-old Nordhordland bridge in Norway." Research Publishing, 2023, Unpublished proceedings of the 33rd European Safety and Reliability Conference.

[2] Norwegian Public Roads Administration, "Ferjefri E39," [Accessed 13.05.2023]. [Online]. Available: https://www.vegvesen.no/vegprosjekter/europaveg/ferjefrie39/

[3] Norwegian Public Roads Administration, "Risikoanalyse - Skipskollisjon Nordhordalandsbrua," 2017.

[4] LSTC, "LS-DYNA keyword user's manual - volume I," 2012.

[5] Y. Capar. Implicit vs explicit approach in fem. [Online]. Available: https://yasincapar.com/implicit-vs-explicit-approach-in-fem/

[6] W. K. M. Frhaan, B. Abu Bakar, N. Hilal, and A. I. Al-Hadithi, "Cfrp for strengthening and repairing reinforced concrete: A review," *Innovative Infrastructure Solutions*, vol. 6, pp. 1–13, 2021.

[7] *Design against accidental loads, DNV-RP-C204*, DNV GL AS, 2017.

[8] G. Gholipour, C. Zhang, and A. A. Mousavi, "Nonlinear failure analysis of bridge piers subjected to vessel impact combined with blast loads," *Ocean Engineering*, vol. 234, 2021.

[9] S. Zhang, P. T. Pedersen, and R. Villavicencio, "Probability of ship collision and grounding," in *Probability and Mechanics of Ship Collision and Grounding.* United States: Elsevier, 2019.

[10] *Laster på konstruksjoner - Ulykkeslaster, NS-EN 1991-1-7*, Standard Norge, 2006.

[11] Norwegian Public Roads Administration, "Construction drawings of nordhordland bridge," 1996, Unpublished.

[12] Norwegian Public Roads Administration, "Nordhordland bridge," 1994.

[13] M. E. Eidem, Personal Communication, 8. March 2023.

[14] S. L. Hafsaas, "Styrmann sovnet - nå må han møte i retten," *NRK*, 2021, [Accessed 26.04.23]. [Online]. Available: https://www.nrk.no/vestland/mann-_26_-ma-i-retten-etter-at-lastebat-kjorte-rett-inn-i-nordhordlandsbrua-1.15685822

[15] B. T. Olsen and B. Vaksdal, "Lastebåt krasjet i nordhordlandsbrua," *Bergensavisen*, 2009, [Accessed 26.04.2023]. [Online]. Available: https://www.ba.no/nyheter/lastebat-krasjet-i-nordhordlandsbrua/s/1-41-4371794

[16] Tornado. MarineTraffic. [Accessed 18.05.2023]. [Online]. Available: https://www.marinetraffic.com/en/ais/details/ships/shipid:311494/mmsi:258260000/imo:7042291/vessel:TORNADO

[17] Framfjord. MarineTraffic. [Accessed 18.05.2023]. [Online]. Available: https://www.marinetraffic.com/en/ais/details/ships/shipid:268153/mmsi:-8913473/imo:8913473/vessel:FRAMFJORD

[18] Nyfjell. MarineTraffic. [Accessed 18.05.2023]. [Online]. Available: https://www.marinetraffic.com/en/ais/details/ships/shipid:311406/mmsi:258221000/imo:7602584/vessel:NYFJELL

[19] M. Lwin, "Floating bridges," in *Bridge Engineering Handbook*, W.-F. Chen and L. Duan, Eds. United States: Taylor Francis, 2014, pp. 549–571.

[20] C. Baum and A. Frostis, "Prognoser for sjøtrafikk 2018 - 2050," 2018.

[21] V. Minorsky, "An analysis of ship collisions with reference to protection of nuclear power plants," Sharp (George G.) Inc., New York, Tech. Rep., 1958.

[22] S. Zhang, "The mechanics of ship collisions," Ph.D. dissertation, Technical University of Denmark, 1999.

[23] G. Woisin, "Design against collision," *Advances in Marine Technology*, 1979.

[24] L. Walter and A. Styhre, "The role of organizational objects in construction projects: the case of the collapse and restoration of the tjörn bridge," *Construction management and economics*, vol. 31, no. 12, pp. 1172–1185, 2013.

[25] G. R. Consolazio, R. A. Cook, M. C. McVay, D. Cowan, A. Biggs, and L. Bui, "Barge impact testing of the st. george island causeway bridge, phase III: physical testing and data interpretation," Tech. Rep., 2006.

[26] P. Yuan and I. E. Harik, "One-dimensional model for multi-barge flotillas impacting bridge piers," *Computer-Aided Civil and Infrastructure Engineering*, vol. 23, no. 6, pp. 437–447, 2008.

[27] Y. Sha and J. Amdahl, "Numerical investigations of a prestressed pontoon wall subjected to ship collision loads," *Ocean Engineering*, vol. 172, pp. 234–244, 2019.

[28] Y. Sha and H. Hao, "Laboratory tests and numerical simulations of cfrp strengthened rc pier subjected to barge impact load," *International Journal of Structural Stability and Dynamics*, vol. 15, no. 02, 2015.

[29] Y. Sha, "Cfrp strengthening of reinforced concrete pontoon walls against ship bow collisions," *Structure and Infrastructure Engineering*, vol. 18, no. 8, pp. 1091–1106, 2022.

[30] G.-R. Liu and S. S. Quek, *The finite element method: a practical course*. Butterworth-Heinemann, 2013.

[31] R. D. Cook, D. S. Malkus, M. E. Plesha, and R. J. Witt, *Concepts and applications of finite element analysis*, 4th ed. New York: Wiley, 2002.

[32] *Determination of Structural Capacity by Non-linear FE analysis Methods, DNV-RP-C208*, DNV GL AS, 2013.

[33] Y. Sha, "Advanced analysis and design of steel structures, lecture 8 - NLFEA for ALS," 2022, University of Stavanger.

[34] DYNAmore Nordic AB, "Introduction to LS-DYNA," 2023, course material.

[35] ANSYS, "LS-DYNA," [Accessed: 12.04.2023]. [Online]. Available: https://www.ansys.com/products/structures/ansys-ls-dyna

[36] DYNAmore Nordic AB, "LS-Prepost," [Accessed: 12.04.2023]. [Online]. Available: https://www.dynamore.de/en/products/pre-and-postprocessors/prepost

[37] P. Fidjestol, "High performance lightweight concrete bridges-norwegian background and experience," in *PCI National Bridge Conference, 3 rd International Symposium on High Performance Concrete*, 2003.

[38] P. T. Pedersen, J. Chen, and L. Zhu, "Design of bridges against ship collisions," *Marine Structures*, vol. 74, p. 102810, 2020.

[39] *Actions and action effects, N-003*, NORSOK Standard, 2017.

[40] Y. Sha, "Advanced analysis and design of steel structures, lecture 6 - ship collision introduction," 2022, University of Stavanger.

[41] C. E. Buth, W. F. Williams, M. S. Brackin, D. Lord, S. R. Geedipally, A. Y. Abu-Odeh *et al.*, "Analysis of large truck collisions with bridge piers: phase 1, report of guidelines for designing bridge piers and abutments for vehicle collisions." Texas Transportation Institute, Tech. Rep., 2010.

[42] P. T. Pedersen, "Review and application of ship collision and grounding analysis procedures," *Marine Structures*, vol. 23, no. 3, pp. 241–262, 2010.

[43] Norwegian Coastal Administration, "About the Vessel Traffic Service (VTS)," [Accessed 01.06.2023]. [Online]. Available: https://www.kystverket.no/en/navigation-and-monitoring/vts---vessel-traffic-service/about-the-vessel-traffic-service-vts/

[44] Y. Huang, L. Chen, P. Chen, R. R. Negenborn, and P. Van Gelder, "Ship collision avoidance methods: State-of-the-art," *Safety science*, vol. 121, pp. 451–473, 2020.

[45] M. E. Eidem, "Analysis for decision support for retrofitting the nordhordland bridge to withstand higher ship impact loads," Norway, 2022.

[46] R. H. Svendsen, "Lastebåt smalt inn i flytebro," *NRK*, 2009, [Accessed 26.04.2023]. [Online]. Available: https://www.nrk.no/vestland/lastebat-smalt-inn-i-flytebro-1.6635517

[47] LSTC, "LS-DYNA keyword user's manual - volume II," 2014.

[48] W. Fan and W. Yuan, "Numerical simulation and analytical modeling of pile-supported structures subjected to ship collisions including soil–structure interaction," *Ocean engineering*, vol. 91, pp. 11–27, 2014.

[49] K. Fujikake, B. Li, and S. Soeun, "Impact response of reinforced concrete beam and its analytical evaluation," *Journal of structural engineering*, vol. 135, no. 8, 2009.